ACKNOWLEDGMENTS

I thank Dr. Parker C. Reist for his personal interest, technical expertise and editorial help throughout my research and studies at Environmental Sciences and Engineering.

I also thank my committee members for their guidance: Donald L. Fox, Richard Kamens and William Wilson.

I am grateful to MANTECH ENVIRONMENTAL SCIENCES in the Research Triangle Park, who provided the initial funding for my studies at UNC, and granted me the time from my job to further my studies.

I am also grateful to the USEPA at the Research Triangle Park for providing partial support through the cooperative agreement No CR822078 with the University of North Carolina at Chapel Hill, School of Public Health.

Last, but certainly not least, I am grateful to my family for their total support and editorial help for this and previous drafts of this report. Their names are my wife Argentina, and my daughters: Lindelly, Julia Argentina and Ixchel Trinidad .

TABLE OF CONTENTS

Page

1. SYMBOLS.....i-ii

2. INTRODUCTION.....1

3. THEORETICAL BACKGROUND.....4

3.1 Basic Assumptions.....4

3.2 Mie Scattering. Extinction Coefficient..... 6

4. RWM Acronym..... 7

4.1 Role played by the Ammonia in the Atmosphere.....9

5.1 Simulation values.....10

5.2 Data Set Used For Program Evaluation.....13

5.3 Verification Studies.....15

5.4 New Results: Crucial Test.....36

6. Visual Air Quality indicator. Relative Visual Index (h_v).....37

6.1 SENSITIVITY STUDIES RELATED TO hv.....42

7. CONCLUSIONS AND RESULTS.....53

8. REFERENCES

9. APPENDIX A: Conversion Factors. Units.

10. APPENDIX B: Acute Effects.

1. INTRODUCTION

This paper reports on a test of the effectiveness of the Reist Wilson Mars (RWM) program to calculate scattering efficiency values of particulate matter formed from chemical reactions in the atmosphere. The test of the program was done in a two level approach taking into consideration the relationship between simulation, theory, and experimental work as described in the methodology section. The first level was designed as an exhaustive test and only after the program satisfied the requirements of this initial test was the second level attempted which was called a crucial test.

Methodology

To test the program in an exhaustive way, major results and hypotheses related to visibility reduction were searched throughout the literature. Then, simulations were run using the RWM program under conditions similar to the ones found in the literature for the specific findings. Finally,

comparisons were done between the RWM results and the previously published results.

To provide a crucial test of the RWM program, simulations of the RWM program under extreme experimental conditions were designed and run. It was found that the simulation itself was able to suggest insights to the experimentalist. This could be used to assist in the interpretation of new results in the behavior of the light scattering coefficients as it relates to the fractional mass concentration.

Relationship between simulated, theoretical and Experimental work

The relationship between theory, experiment and simulated work is better explained through a block diagram (FIG.A). Since the 1980's when the PC came in full force, scientists have been replacing the proverbial "thought experiment" with "virtual experiments". Today experiments are "performed" and answers are obtained using a computer program. In this way, computer simulation is a test of a theory, and it is hoped that a good simulator can discriminate between a well-founded approach to a problem and merely a speculative suggestion of a less than plausible outcome. In this technical report it was one of our aims to develop a crucial test for the simulation, where crucial was meant to be a new or not yet found result that could give experimentalists and

theorist alike some job to do. The simulator is a bridge between the theory and the experiment, making the theory more accessible to experimentalist and vice versa.

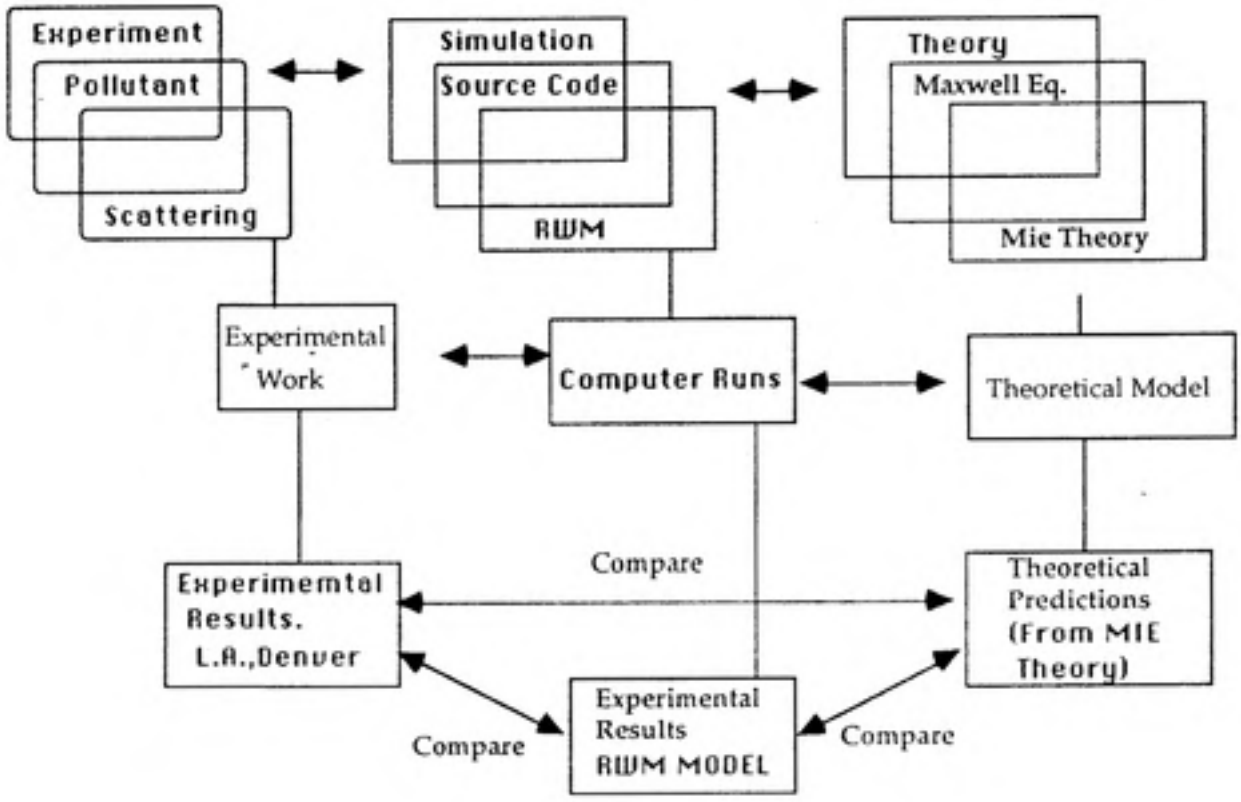


FIG.A. Block diagram showing the relationship among the different elements that are considered in this technical report: The experimental work, the RWM simulator and the MIE scattering theory.

3. THEORETICAL BACKGROUND

Visibility reduction is due to the interaction of light with matter, giving rise to absorption and scattering. The results of this technical report will be based on the framework of the Mie scattering theory, which predicts the interaction of light with small particles.

This report then rests on Mie's theory basic assumptions [38]:

3.1 Basic Assumptions

The basic assumptions associated with MIE theory are as follows:

i) Elastic interaction between light and matter.

ii) Independence of the particles.

iii)Single Scattering.

iv) Sphericity of the particles.

v) The same index of refraction for all the aerosol. These assumptions are discussed in more detail below:

i) All the interaction of light with matter is elastic. The incoming and outgoing photons have the same frequency f'=f. Inelastic scattering takes place when there is some electron transition between energy levels giving rise to Raman scattering and other quantum effects. The spectrum

of the visible radiation that this report deals with does not have enough energy to produce inelastic scattering. Thus, this is a valid assumption for the interaction of visible light with aerosols.

ii) The distance between the particles is greater than 3 times the radius. The radiation of one particle is independent from another one. The phase relation among the different scattering centers is random. This means that there is not a phase or a cooperative effect. A cooperative effect is one that takes place when phase coherence phenomena occurs. This is also a valid assumption.

iii) The effects of multiple scattering will be neglected. This is the most restrictive assumption, since with observed results in the atmosphere there usually is multiple scattering. If the optical depth ($\tau=\sigma_e x$), is less than 0.1($\tau<0.1$) single scattering prevails [38]. This corresponds to cases where the ratio of $I/Io>0.9$. In the expression $\sigma_e x$, σ_e is the cross section extinction coefficient, and x is the optical distance travelled by the light beam. If the optical depth is between 0.1 and 0.3 ($0.1<\tau<0.3$), corresponding to $0.90 > I/Io > 0.74$, it may be necessary to make corrections for double scattering [38].

iv) Extinction coefficients by regularly and irregularly shaped particles have been reported in the literature [10]. The RWM program does not consider these cases. It only takes into consideration spherical particles. For the size of the particles being considered, which are of the same order of magnitude as the visible light, the shape of the particle might not have a very profound effect. Since $x= \pi d/\lambda=1$, the wavelength of the visible light will envelope the entire particle.

v) All aerosol particles have the same index of refraction. This assumption is also a bit restrictive since the different aerosol compounds have indexes of refraction in the range of 1.2 to 1.72.

3.2 Mie Theory. Extinction Coefficient.

The extinction coefficient for a single particle of radius r is given by Van de Hulst [38],pp 127 as:

$$(1) \quad \sigma_{ep} = \pi r^2 Q_e$$

where Q_e is the efficiency factor developed by Mie using electromagnetic theory for the incident wave being scattered by a spherical homogeneous particle. The efficiency factor Q_e depends on the size parameter x

($x=\pi d/\lambda$), and on the index of refraction m'. The value of the index of refraction is $m' = n - ki$ where the real part represents scattering and the imaginary part represents a small contribution due to absorption. The efficiency factor Qe calculated from Mie theory is a function of an infinite sum over Legendre polynomials $P^1_n(\cos\theta)$ and Bessel functions $J_n(kr)$ ([38],pp 121). In order to carry out this investigation, the efficiency factors, and extinction coefficients were computed from the Mie equation using the RWM program. The RWM program computes the Mie equation for individual aerosol particles and calculates the values of the efficiency factors Qe. The program also calculates the values of the extinction coefficients for a polydisperse particle system under a variety of atmospheric and particle characteristics which are described in the next section.

The extinction coefficient for a polydisperse system is:

$$(2) \quad be = \int \pi r^2 Qef(r)dr$$

Since for every simulation, the RWM program computes the TSP (total suspended particle) in units of mass per volume (μg/m3), The mass extinction coefficient was found from:

$$(3) \quad bme = be/TSP$$

4. RWM Acronym

The RWM program is a Mie scattering program originally written by Reist [28], combined with the MARS (Model for an Aerosol Reacting System) program, originally developed by Saxena et al. [30]. F. Binkowski and M. Gary [2] are the modifiers of the original program . Combination of the MARS program with a Mie scattering program to compute the extinction coefficients for various aerosol configurations was carried out by Wilson and Reist [28]. Throughout this paper, the combined Mie scattering-modified version of the MARS program will be denoted by the initials RWM. The original MARS program "predicts the quantity and composition of secondary atmospheric aerosols containing sulfate, nitrate and ammonium compounds" [30]. The program allows the user to input an aerosol phase of sulfate, nitrate and/or ammonium ions in units of $\mu g/m^3$, and a gas phase of ammonia, nitric acid and sulfuric acid in a concentration of ppb. The program also allows the user to choose the relative humidity, temperature and the atmospheric pressure. The RWM program simulates the Mie equation for individual aerosol particles and computes values of the efficiency factors. The program also calculates values of the extinction coefficients for a

polydisperse aerosol under a variety of conditions. The conditions can be chosen from a menu provided by the program which includes the choice of 5 different size distributions from the log-normal, the bimodal log-normal, the Junge, an EPA size distribution, or a user provided distribution. The user can also choose the values of the geometric mean diameter and of the geometric standard deviation, as well as the value of the index of refraction, wavelength of light, and whether the original aerosol represents the size distribution before or after humidification.

4.1 Role played by the ammonia in the atmosphere.

The sulfuric and nitric acid are neutralized by the ammonia present in the atmosphere. The modified version of the MARS program also simulates the equilibrium reactions between the H_2SO_4, HNO_3 and NH_3. To have a better understanding of this modified program the program was run under similar conditions as Saxena et al [30].

An ammonia deficient environment was first simulated, where $[NH_3] \leq 2[H_2SO_4]$, then an ammonia rich environment was run, where $[NH_3] \geq 2[H_2SO_4]$, where [ ] represents the molar concentration.

The gas phase concentrations used for the ammonia deficient and ammonia rich atmospheres were:

ß =(NH_3,HNO_3,H_2SO_4)= (10,25,25) ppb, NH_3 deficient.

- ß =(NH_3,HNO_3,H_2SO_4)= (50,25,25) ppb, NH_3 rich.

It is suggested that future runs should be done with the following concentrations:

ß. =(NH_3,HNO_3,H_2SO_4)= (100,25,25) ppb, NH_3 rich.

5.1 Simulation Values.

Three major parameters impact on the RWM program simulations.

- Atmospheric characteristics of Pressure, Temperature, Relative Humidity, and the Wavelength of light.
- The aerosol's physical characteristics which includes particle size, geometric standard deviation, and size distribution function.
- The aerosol's chemical characteristics of index of refraction as a chemical differentiator, and concentration of the different pollutants.

In order to run the simulations, it was necessary to choose values for all parameters given in the program, which were taken to be most representative of a typical urban atmosphere:

- Pressure = 1 atmosphere.
- Temperature = 298 ^{O}K.
- Low relative humidity case:50 %. High relative humidity case :90 %

- Wavelength of the light, λ = 0.55 µm.

Aerosol:

- Size Distribution function: Log-Normal
- Geometric mean particle diameter by count: d_g = 0.4 µm
- Mass mean particle diameter : d_{mmd} = 0.5 µm (σ_g=1.25)
- Geometric Standard Deviations: 1.2,1.25,1.5,1.72
- Aerosol index of refraction: m'=1.5-0.01i
- Aerosol phase: $NH4^+$ = 10 µm/m^3, $NO3^-$ = 10.7 µm/m^3, $SO4^=$ = 13.5 µm/m^3

- Gas phase for an ammonia rich environment:

  NH_3 = 50 ppb, HNO_3 = 25 ppb, H_2SO_4 = 25 ppb

- Gas phase for an ammonia deficient environment:

  NH_3 = 10 ppb, HNO_3 = 25 ppb, H_2SO_4 = 25 ppb

Reasoning behind the choice of values.

A Pressure of 1 atmosphere was chosen since some of the experimental work used for comparison was done at sea level and not much error is introduced by keeping this value throughout. The Temperature of 298 °K was chosen following the work by Saxena et.al. [30]. The values for the low and high relative humidity were chosen following the work of Cass et.al [3].The wavelength of 0.55 µm was chosen for several reasons. First, this value is given by default by the RWM program, second the wavelength of 0.55 µm is the wavelength

of maximum response to the human eye. Finally this value is the mean value of the wavelength range for visible light: 0.4-0.7 μm. The Log-Normal Distribution was chosen based on a work by Waggoner [39], and on theoretical considerations by Raabe [27] and Crump [5]. Raabe suggests that Nature's phenomena are Log-normally distributed, Crump's choice of the Log-Normal distribution is based on its mathematical properties. Crump's claims that the Log-Normal distribution lies in the Hilbert Space, and as such, it can be written as a linear combination of orthonormal quantities. He uses this function to solve the inverse size distribution problem, getting very good agreement between the experimental and theoretical results when a Log Normal size distribution is used. The geometric mean particle diameter by count, 0.4 μm, was chosen for two reasons: First, according to Mie theory, the peak in the light scattering efficiency occurs when the ratio $\pi dg/\lambda = 1$. Second, when doing the initial runs, a graph of b_{ms} versus dg gave a peak at a value of dg equal to 0.4 μm. The choice of the values used for the geometric standard deviation was based on two aspects. For a Log-Normal size distribution, 95% of all the particles lie in the range $d_g/2\sigma_g$ to $d_g*2\sigma_g$ [29].So having chosen d_g = 0.4 μm, and the range of 0.1 to 1.0 μm as the most optically active region, it was found that for d_g=0.1, σ_g =1.25, and for d_g = 1,σ_g =2. The second reason behind the choice of values for σ_g was due to a work by Middleton [19]. The index of refraction was chosen following a work by H.Horvath [9], and with the

objective of being able to simulate the different chemical components in the atmosphere. The aerosol and gas phases were chosen following Seinfeld [31] and the work of Cass [2].

5.2 Data Sets Used For Program Evaluation.

TABLE I gives the concentrations in units of μg/m3 and ppb for a clean and for a polluted atmosphere according to Seinfeld [31]. The actual values used to run the simulations were taken from two previously published works: Cass [2] and Saxena et al.[30]. The values used are within the ranges set forth by Seinfeld. Simulations were done to account for "clean" air and polluted air. In the Denver area studies [7,13] the main polluters are soot and sulfates. In the Los Angeles area studies [2,42] the main polluters are sulfates and nitrates. Soot was simulated using inert aerosol and an index of refraction of m'=2.0 - 1i. Sulfates were simulated with the inert aerosol equal to zero and using m'=1.5-0.01i. The RWM program has two phases:

An aerosol phase denoted by:

$$\alpha=(NH_4^+, NO_3^-, SO_4^=), \text{ and}$$

A gas phase denotated by :

$$\beta = (NH_3, HNO_3, H_2SO_4)$$

The aerosol phase is given in the RWM program in units of μg/m3, and the gas phase in units of ppb. Not all references agreed on the units. To have a verification of

results, a conversion factor between the two sets of units is shown in APPENDIX A.

TABLE I: Trace Species concentrations in the clean troposphere and polluted urban air ([29],pp1, pp 37,pp41).

(I) Gas phase

Species	Concentration in ppb	
	Clean Troposphere	Polluted Air
NH_3	1	10-25
HNO_3	0.02-0.3	3-50
H_2SO_4	1	20

	Concentration in $\mu g/m^3$	
	Clean Troposphere	Polluted Air
NH_3	0.7	7-17.4
HNO_3	0.05-0.8	8-130
H_2SO_4	3.5	8.1

(II) Aerosol phase

Species	Concentration in µg/m3	
	Clean Troposphere	Polluted Air
NH_4+	0	2.38
NO_3-	0	4.76-31.5
$SO_4=$	0.5	10.7-11.58
TSP	5-25	70.5-250

Cass and Saxena Data Sets [2,30]

Aerosol phase as obtained from data encountered in reference [2] was used,

$\alpha = (NH_4+, NO_3-, SO_4=) = (10, 10.7, 13.5)$ µg/m3

Gas phase as obtained from Seinfeld's book and concurrently from Saxena et al. reference [30] was used throughout this technical report.

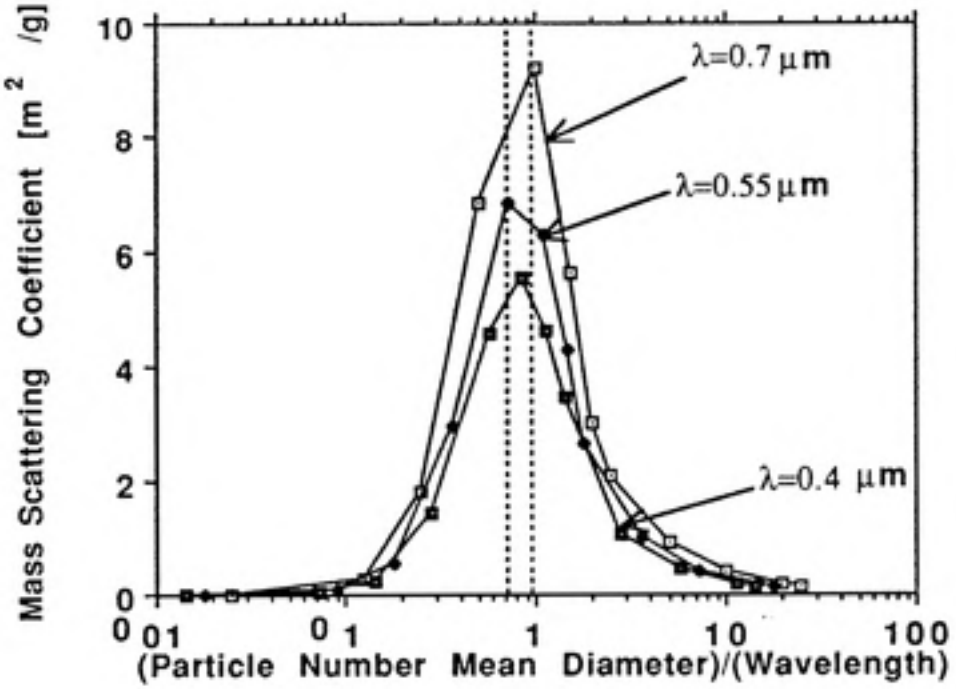
$\beta = (NH_3, HNO_3, H_2SO_4 = (50, 25, 25)$ ppb, ammonia

rich environment
β = (10,25,25) ppb ammonia deficient environment

5.3. VERIFICATION STUDIES

The mass scattering coefficient reaches a peak at $\pi dg/\lambda = 1$ as shown in Fig.1. This confirms the experimental and theoretical results related to the maximum optical effects occurring when the particle diameter is of the same order in size as the wavelength of the incident light. As the wavelength of light increases from 0.4 to 0.7 μm, the peak of the mass scattering coefficient increases. According to this result blue light is less sensitive to scattering and red light most sensitive to scattering by aerosols in the atmosphere.

Experimental investigations have shown that atmospheric size distributions are multimodally distributed. Waggoner et.al. [39] give a three mode distribution, which they called nuclei, accumulation, and coarse modes with typical mass mean diameters of 0.03, 0.3 and 20 μm respectively. For optical effects, some investigators have found [8,31] that particles in the size range from 0.1 to 1.0 μm, that is, particles in the accumulation mode, are the most active when irradiated with visible light. The result of the RWM simulation confirm these findings



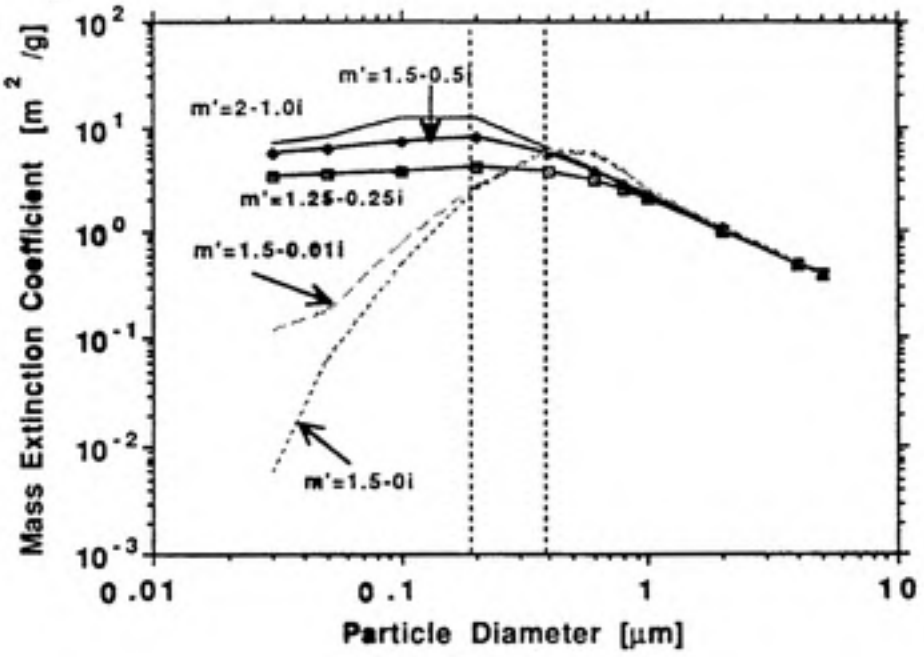
Input Conditions on RWM Simulator to obtain Fig.1:

m'=1.5-0.01i
Wavelength of light: 0.4,0.55 and 0.7 μm
Geometric Standard Deviation: 1.25
Size Distribution: Log-normal
α = (10,10.7,13.5) μg/m3
β = (50,25,25) ppb
T = 298 oK, P = 1 atm., RH = 90%

Fig. 1 Mass Scattering Coefficient as function of the ratio of particle number mean diameter to wavelength of light. The peak occurs in the range corresponding to the wavelength of the scattered light particle size range.

as seen in (Figures 1,2, and 4). Mass absorption coefficients are constant for particles less than 0.1 μm and are inversely proportional to the particle size for particle sizes greater than 1 μm. For comparison, inset 1 show results similar to the ones found in Fig.2. Both results agree in the optically active region. In both Figures, the maximum mass scattering coefficient occurred at a particle diameter by count of 0.4μm. Using the Hatch-Choate relationship: $\log d_{mmd} = \log d_g + 8{,}05 * \log^2 \sigma_g$, and $\sigma_g = 1.25$, this corresponds to a mass mean diameter of $d_{mmd} = 0.5$ μm. The optical range using mass mean diameter is from 0.1 to 1.2 μm, which is not much different from the optically active region using particle diameter by count. The reason behind this near equality in the optically active region of particle diameter by count and by mass is the value chosen for the geometric standard deviation.

A very good fit was found between the simulated results from the RWM program for the scattering coefficient as a function of the relative humidity as seen in Fig. 3, and the theoretical expression developed by Zhang X.Q.as reported in reference [11]. This reference shows experimental results for the light scattering efficiency as a function of relative humidity that



Input Conditions on RWM Simulator to obtain Fig.2:

Wavelength of light:0.55 μm
Geometric Standard Deviation: 1.5
Geometric mean particle size:0.4 μm
Size Distribution: Log-normal
T = 298 oK, P = 1 atm., RH = 63%

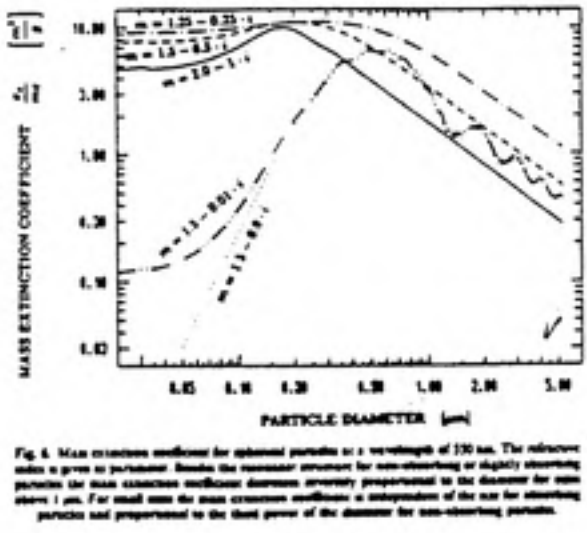
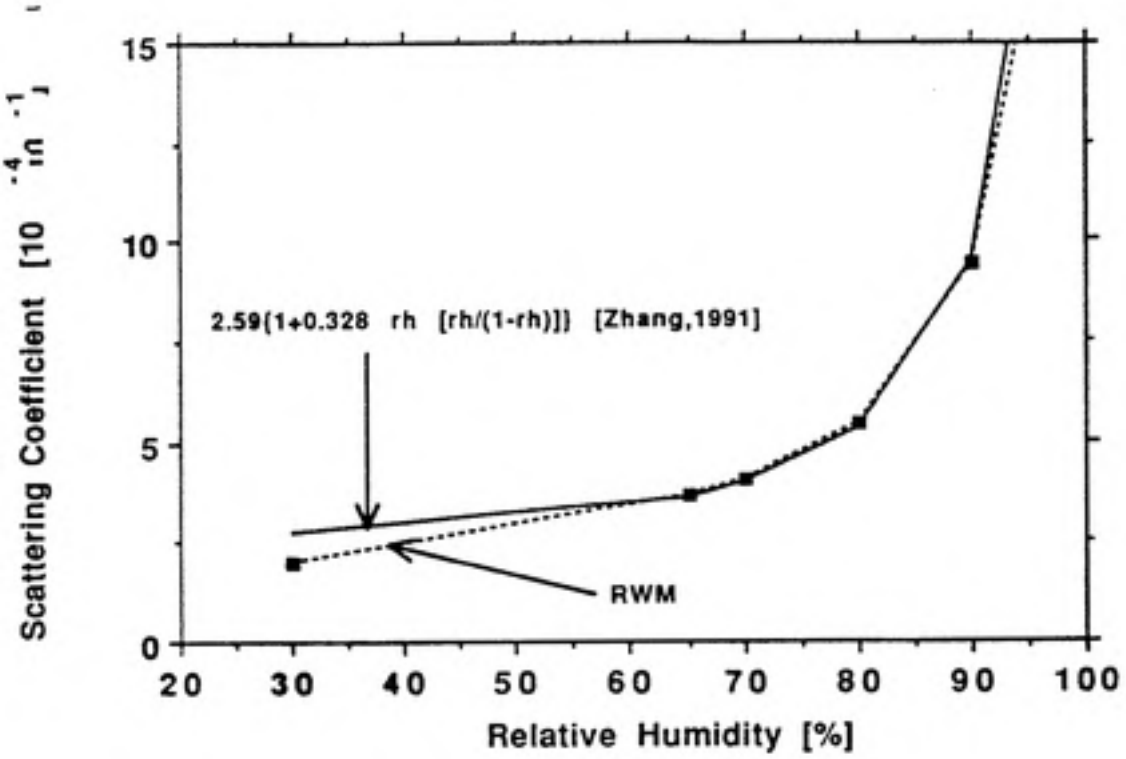


Fig. 2 Mass extinction coefficient as function of particle diameter, for different values of index of refraction. The peak occurs in the range corresponding to the accumulation mode size range.



Input Conditions on RWM Simulator to obtain Fig.3:

Index of refraction, m': 1.5-0.01i.
Wavelength of light: 0.55 µm
Geometric Standard Deviation: 2.08
Geometric mean particle size :0.4µm
Size Distribution: Log-normal
α = (10,10.7,13.5) µg/m3
B = (50,25,25) ppb
T = 298 oK, P = 1 atm., RH = 90%

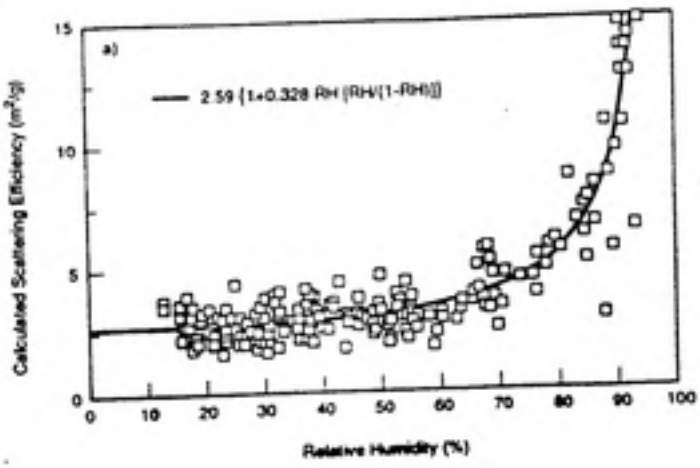
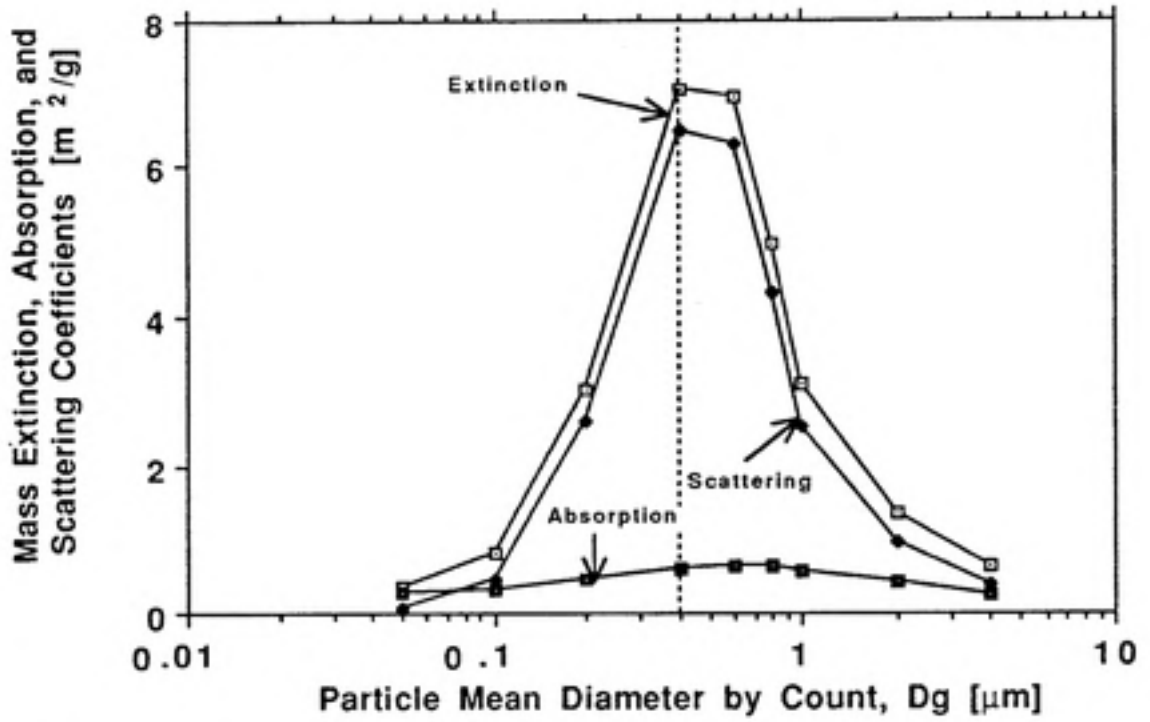


Fig. 3 Scattering Coefficients as function of Relative Humidity.

follows the trend of Fig.3 as seen in inset 2. It is to be noted that the RWM results and the results reported in ref [11] are in agreement only if the vertical axis in ref [11] refers to the light scattering coefficient. Fig.4 confirms the basic relationship between the light scattering, light absorption, and light extinction coefficients. As mentioned above, it was found that the peak for the extinction coefficient occurs in the accumulation or fine mode particle size range. Particles smaller than 0.1 μm, and particles larger than 1 μm, make very small contributions to scattering. Notice that in the lower end of the scale in particle diameter, for particles smaller than about 0.075 μm, in the nuclei mode, the mass absorption coefficient is greater than the mass scattering coefficient.

According to Waggoner et al [39], Horvath and Charlson in their 1968 paper showed that particles in the 0.1-1.0 μm would dominate the scattering given the Junge Power law size distribution. Using the RWM program, it was found that particles in the 0.1 -1.0 μm size range also dominates the scattering given the log-normal size distribution (see Fig.1,2 and 4).

The peak value of the mass scattering coefficient takes place for a range of geometric standard deviation between 1.2 and 1.4., as shown

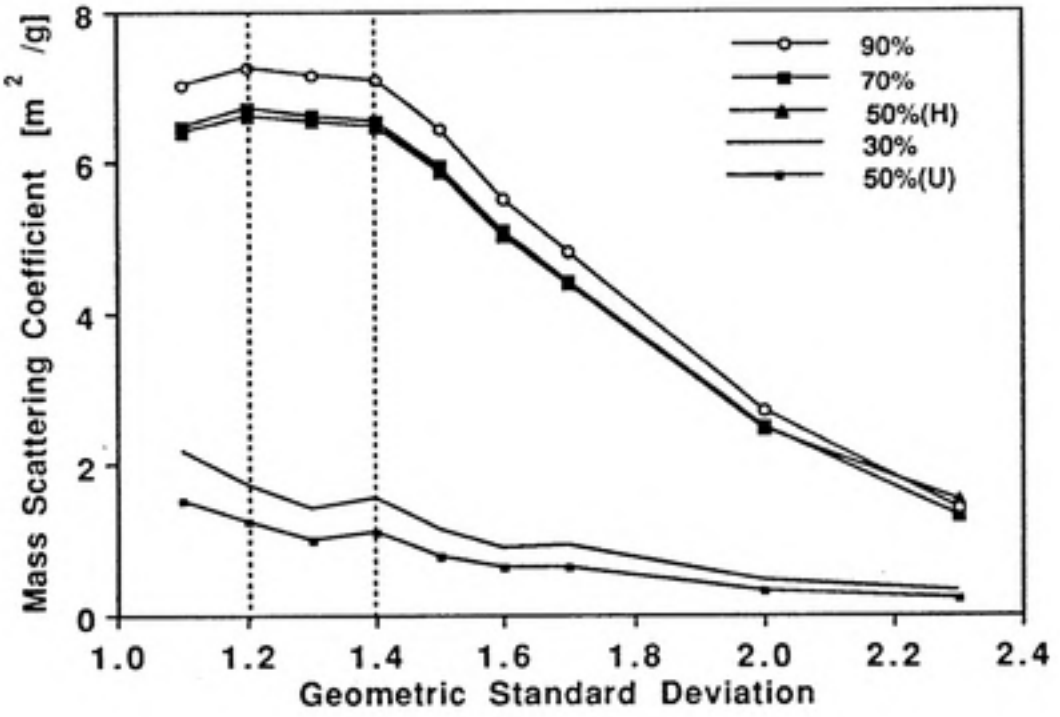


Input Conditions on RWM Simulator to obtain Fig.4:

Index of refraction, m': 1.5-0.02i.
Wavelength of light: 0.55 μm
Geometric Standard Deviation: 1.25
Size Distribution: Log-normal
α = (10,10.7,13.5) μg/m3
β = (50,25,25) ppb
T = 298 oK, P = 1 atm., RH = 90%

Fig. 4 Mass Extinction, Absorption and Scattering Coefficients as function of particle diameter. The peak for the aerosols occurs in the range of 0.4 to 0.6 μm. It was found that bep=bsp+bap.

in Fig.5. Also as seen on Fig.5, the aerosol makes a negligible contribution to the mass scattering coefficient for values of the geometric standard deviation greater than 2. This can be explained as follows. When the particle size dispersion is greater than two, the particle size range goes into the coarse mode which does not make a big contribution to the optical activity. The coarse mode is reached, since in a log-normal size distribution 95 % of its aerosol lies in the range $dg/2\sigma g$ to $dg*2\sigma g$, and if we choose 1 µm for dg, and two for σg we get a range between 0.025 to 4 µm. On the other hand at high relative humidities, when the geometric standard deviation is less than 1.2 the mass scattering coefficient decreases. For low relative humidities the mass scattering coefficient keeps increasing with lowering geometric standard deviation. At high relative humidities the particles grow in size and even if the geometric standard deviation is lower, the mass mean diameter bring the particles over the accumulation mode and over the coarse mode where the optical effect is less pronounced.



Input Conditions on RWM Simulator to obtain Fig.5:

Index of refraction, m': 1.5
Mean particle diameter (by count)=0.4 µm
Wavelength of light: 0.55 µm
Size Distribution: Log-normal
α = (10,10.7,13.5) µg/m3
β = (10,25,25) ppb
T = 298 oK, P = 1 atm., RH = (30-90)%
Humidified & Unhumidified.

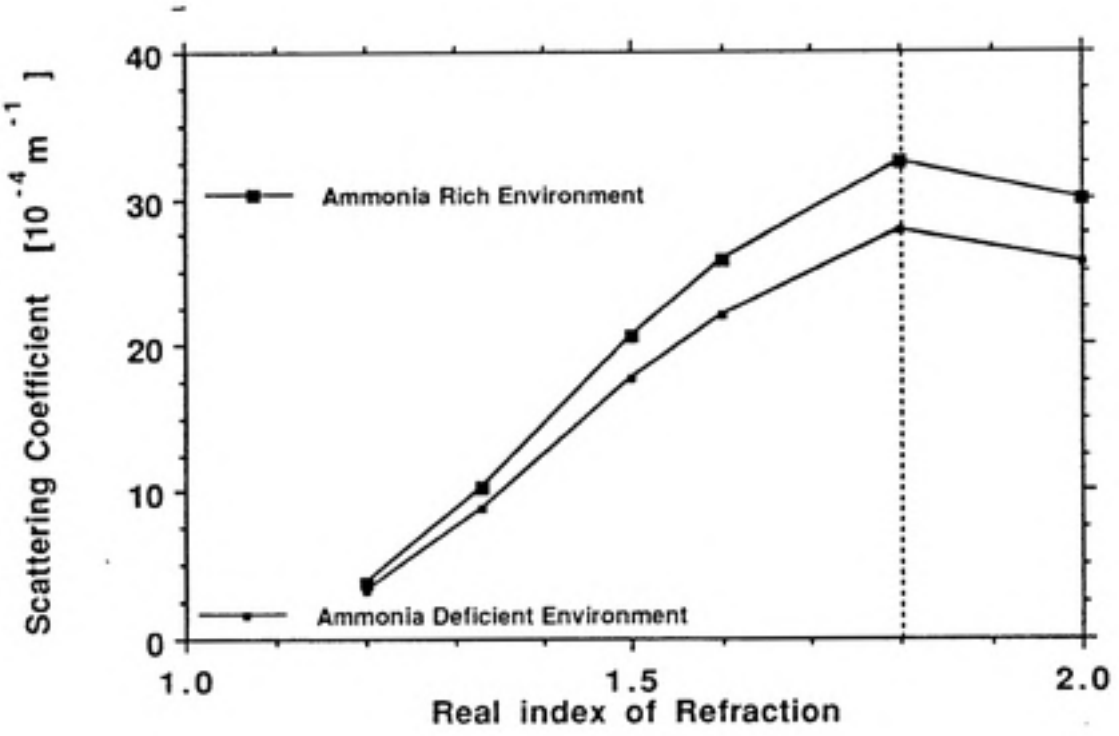
Fig. 5 Mass Scattering Coefficients as function of Geometric Standard Deviation. The peak for the mass scattering coefficient occurs in the range of 1.2 to 1.4.

It was found that the peak value for the scattering coefficient as a function of a real index of refraction occurs at about 1.8 as shown in Fig. 6. For most of the simulations done in this report, the real part of the index of refraction chosen was the bulk value for sulfates, i.e. 1.5. For the range of indexes of refraction between 1.2 to 1.8, the value of the light scattering coefficient is a monotonically increasing function of the index of refraction. This means that sulfates will make a greater contribution to the light scattering coefficient than water, ammonia and nitrates, since they have a greater index of refraction

From measurements of aerosol mass and light scattering at various locations, Charlson et al.[4] found empirically the relationship

(4) $V[m]*TSP[\mu g/m3] \approx 1.2\ g/m^2$

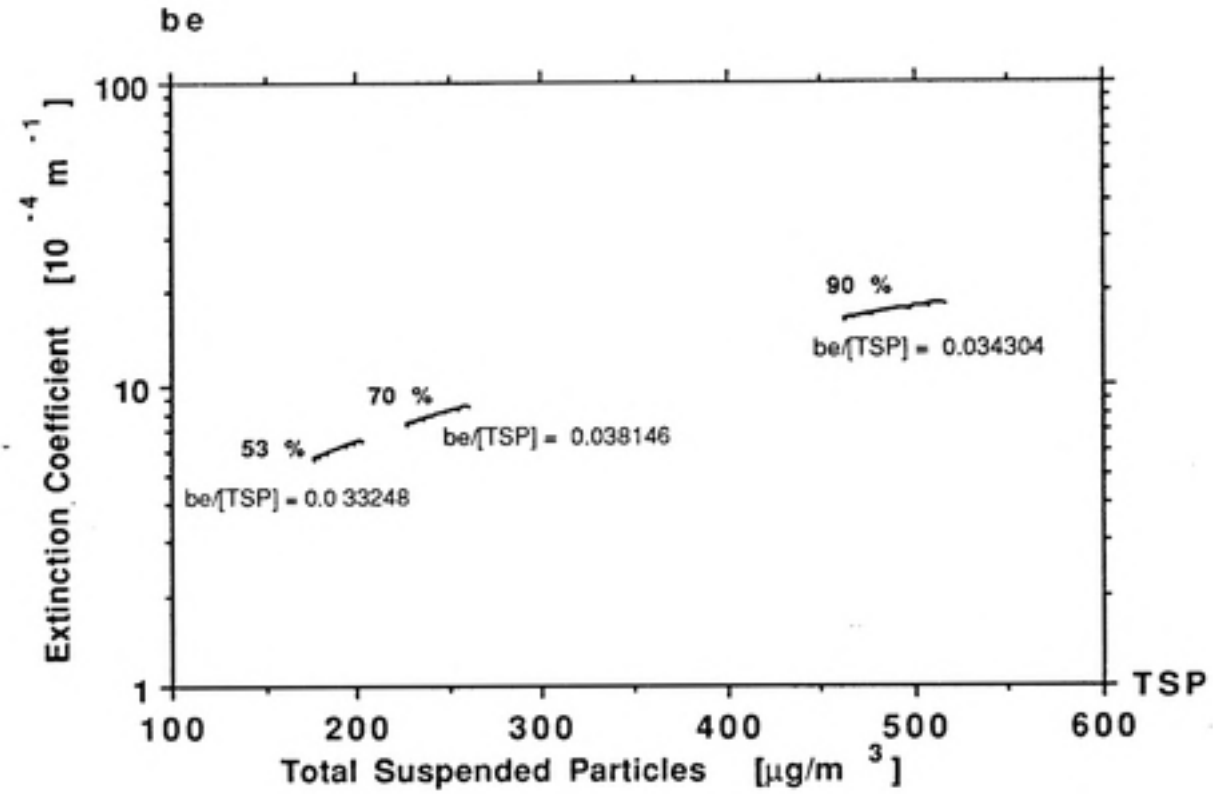
Using the RWM simulations it is found, that at a relative humidity of 53%, be/TSP = 3.32 m2/g (Fig. 7). Using the Koschmieder relationship, it is found that V[m]*TSP[µg/m3]=1.2 g/m2, in good agreement with the empirical relationship mentioned above. From theoretical considerations, Lewis [12] found the relationship be/Mf=3.1



Input Conditions on RWM Simulator to obtain Fig.6:

Index of refraction range, m': 1.2-2.0
Mean particle diameter (by count)=0.4 μm
Wavelength of light: 0.55 μm
Size Distribution: Log-normal
α = (10,10.7,13.5) μg/m3
β = (NH3,25,25) ppb
T = 298 oK, P = 1 atm., RH = 70%
NH3=10,50 ppb

Fig. 6 Scattering Coefficients as function of real index of refraction, m'. The peak for the scattering coefficient occurs for the value of m'=1.8.



Input Conditions on RWM Simulator to obtain Fig.7:

Index of refraction, m': 1.4
Mean particle diameter (by count)=0.5 µm
Geometric StandardDeviation:1.25
Wavelength of light: 0.55 µm
Size Distribution: Log-normal
α = (10,10.7,13.5) µg/m3
B = (10,25,25) ppb
T = 295 oK, P = 1 atm., RH = 70%

Fig. 7 Extinction Coefficient as function of Total Suspended Particles.

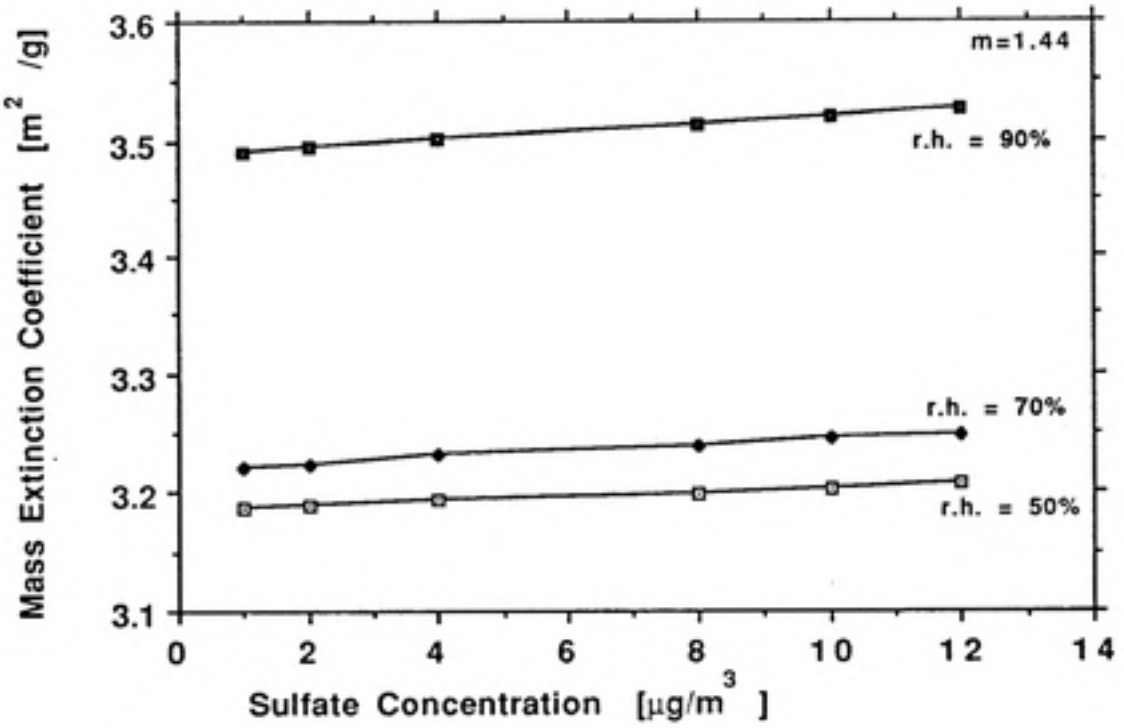
m2/g , when only the fine mass is taken into account. Using the Koschmieder relationship V=3.91/be, it is found that V*Mf = 1.2. This result implies that in the empirical relationship found by Charlson, TSP might really be the optically effective aerosol fine mass (Mf). If this is the case, there will be a very good agreement between theory, experiment and simulation.

Fig.8 shows the mass extinction coefficient as a function of the sulfate mass concentration. The mass extinction coefficient was calculated by the ratio of the extinction coefficient to the total aerosol mass, including water. The mass extinction coefficient increases with an increase in the concentration of sulfate in the atmosphere, in an ammonia rich and in an ammonia deficient atmosphere.

Fig.9 shows the extinction coefficient as a function of the nitrate mass concentration inserted into the model. The extinction coefficient remains constant as expected. In the NH3 deficient atmosphere there will not be any nitrate left. All nitrate will be transformed chemically to nitric acid vapor at equilibrium.

Fig.10 shows the extinction coefficient as a function of the carbon mass concentration. The extinction coefficient increases with an increase in the concentration of carbon in the atmosphere, in an ammonia rich and in an ammonia deficient atmosphere.

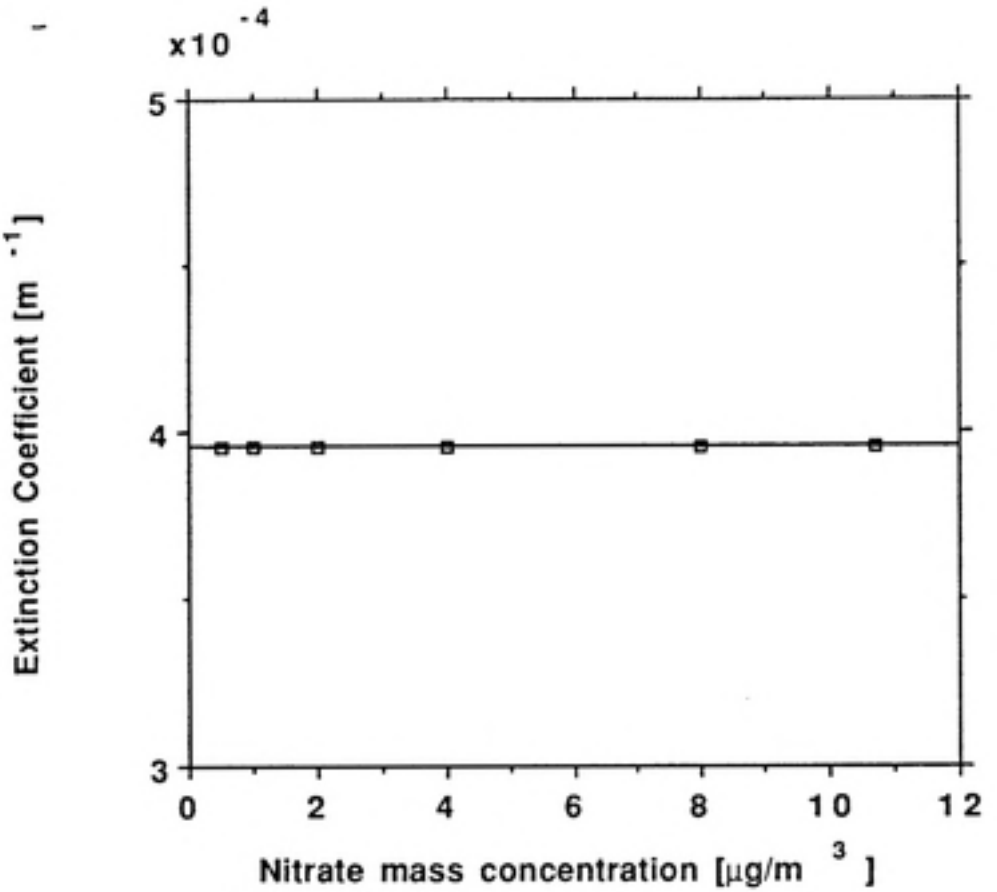
Fig.11 shows the scattering coefficient as a function of increase of ammonium concentration in the model.



Input Conditions on RWM Simulator to obtain Fig.8:

Index of refraction, m': 1.4
Mean particle diameter (by count)=0.5 µm
Geometric StandardDeviation:1.72
Wavelength of light: 0.55 µm
Size Distribution: Log-normal
α = (10,10.7,SO4) µg/m3
B = (10,25,25) ppb
T = 295 oK, P = 1 atm., RH = 70%

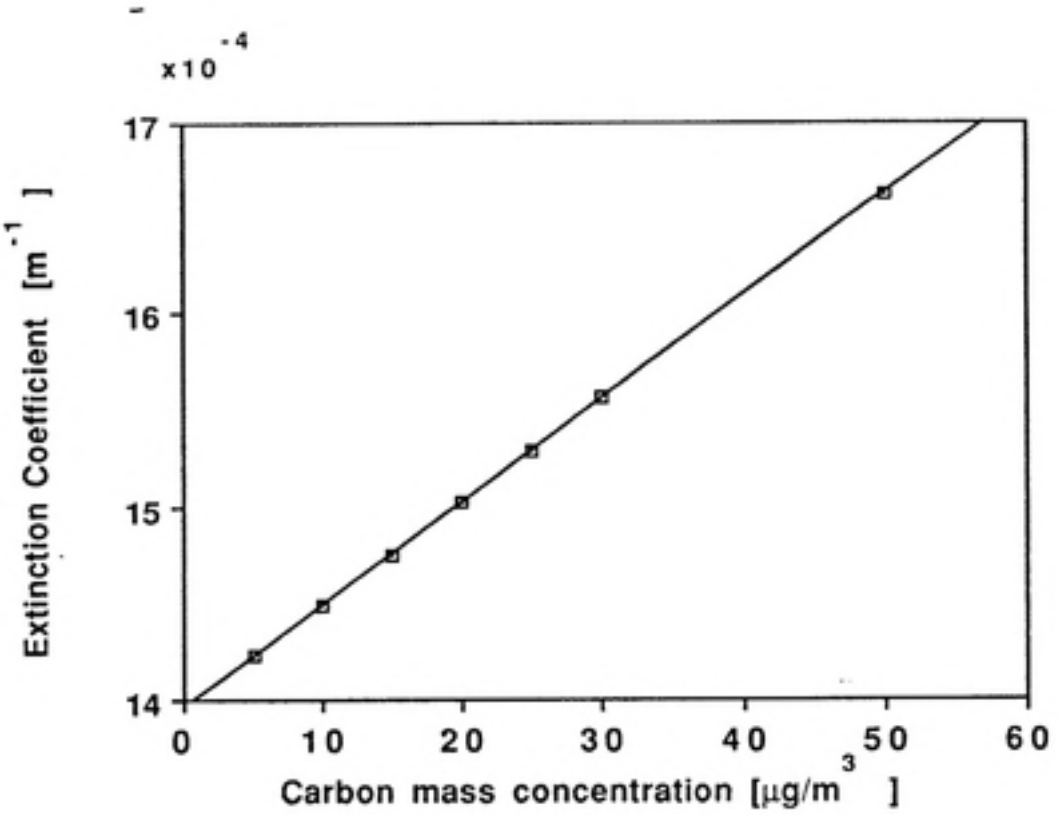
Fig. 8 Mass extinction coefficient as function of sulfate concentration for different values of relative humidity. NH3 deficient environment.



Input Conditions on RWM Simulator to obtain Fig.9:

Index of refraction, m': 1.2
Mean particle diameter (by count)=0.5 µm
Geometric Standard Deviation:1.5
Wavelength of light: 0.55 µm
Size Distribution: Log-normal
α = (10,NO3-,0.5) µg/m3
β = (10,25,25) ppb
T = 295 oK, P = 1 atm., RH = 50%

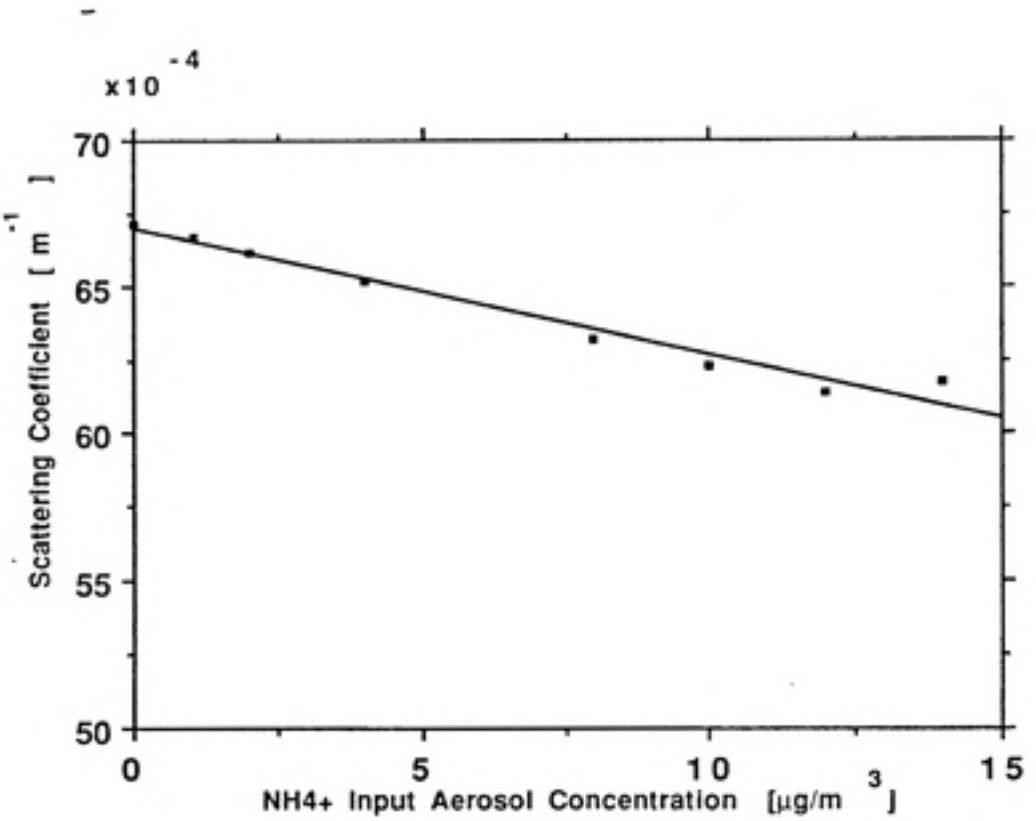
Fig. 9 Extinction coefficient as function of nitrate concentration . NH3 deficient environment.



Input Conditions on RWM Simulator to obtain Fig.10:

Index of refraction, m': 2.0-1.0i
Mean particle diameter (by count)=0.5 µm
Geometric Standard Deviation:1.5
Wavelength of light: 0.55 µm
Size Distribution: Log-normal
α = (10,10.7,13.5) µg/m3
β = (10,25,25) ppb
T = 295 oK, P = 1 atm., RH = 70%

Fig. 10 Extinction coefficient as function of Carbon concentration . NH3 deficient environment.



Input Conditions on RWM Simulator to obtain Fig.11:

Index of refraction, m': 1.5
Mean particle diameter (by count)=0.4 µm
Geometric Standard Deviation 1.2
Wavelength of light: 0.55 µm
Size Distribution: Log-normal
α = (NH4+,0,13.5) µg/m3
β = (10,25,25) ppb
T = 295 oK, P = 1 atm.
RH = 95 %

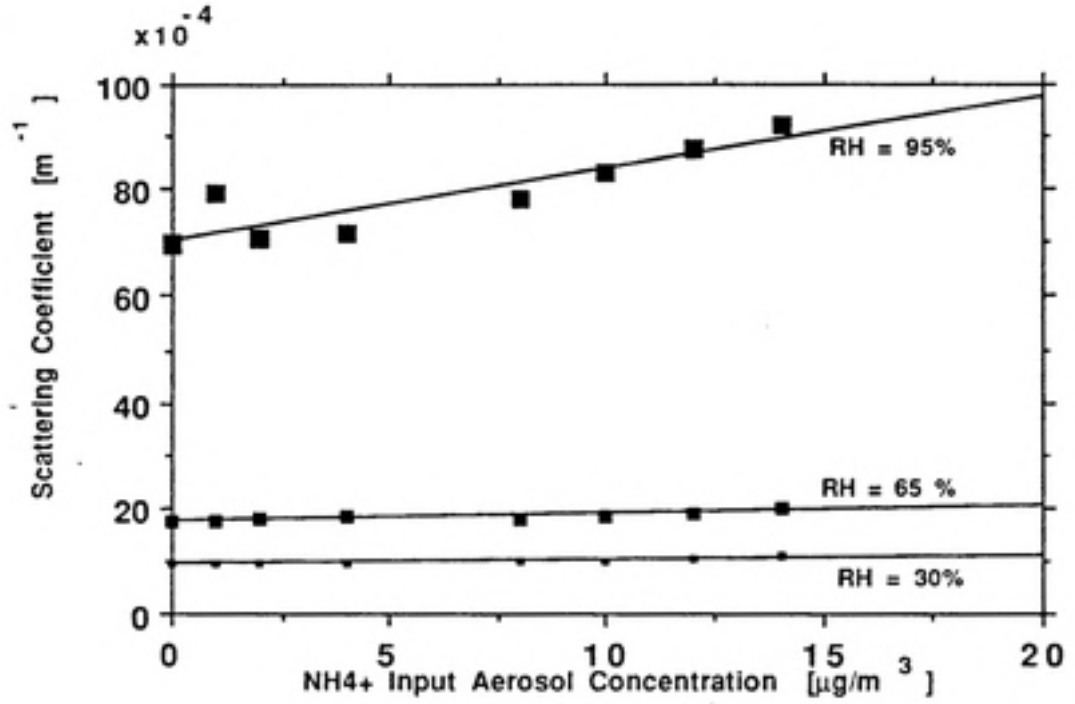
Fig. 11 Scattering coefficient as function of NH4+ aerosol concentration for an ammonia deficient environment.

The scattering coefficient *decreases* with an increase in the concentration of ammonium in the model. This results holds true in an ammonia deficient atmosphere. As the NH4+ is added to the model into the H_2SO_4 aerosol, the sulfuric acid is replaced with NH_4HSO_4 or the NH_4HSO_4 with $(NH_4)_2HSO_4$.

Fig.12 shows the scattering coefficient as a function of increase of ammonium mass concentration in the model. The scattering coefficient increases with an increase in the concentration of ammonium in the model. This result holds true in an ammonia rich atmosphere.

Fig.13 shows the scattering coefficient as a function of increase of ammonium concentration in the model. The scattering coefficient *decreases* with an increase in the concentration of ammonium in the model up to a mass concentration found to be 12 µg/m3, beyond this value the scattering coefficient increases as expected. This result holds true in an ammonia deficient atmosphere.

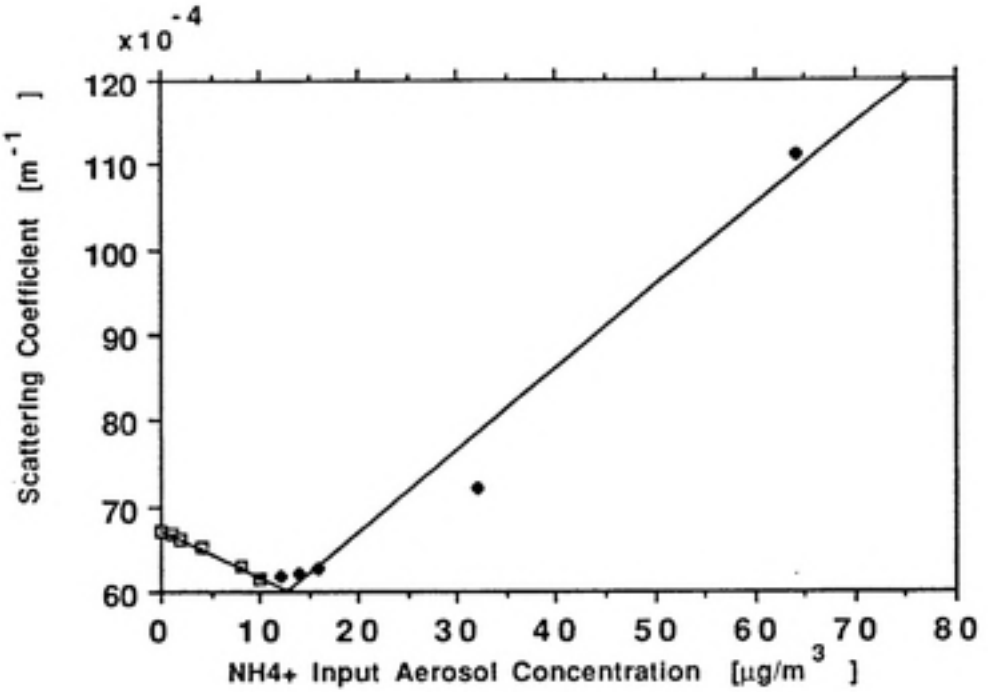
Fig.14 shows the scattering coefficient as a function of increase of ammonium concentration in the model. The scattering coefficient increases with an increase in the concentration of ammonium in the model. This results holds true in an ammonia rich atmosphere. The rich NH3 system has enough NH3 to make (NH4)2SO4 from the gas phase. As NH4+ is added to the model the nitric acid gas is converted to ammonium nitrate aerosol increasing the scattering.



Input Conditions on RWM Simulator to obtain Fig.12:

Index of refraction, m': 1.5
Mean particle diameter (by count)=0.4 µm
Geometric Standard Deviation 1.2
Wavelength of light: 0.55 µm
Size Distribution: Log-normal
α = (NH4+,0,13.5) µg/m3
β = (50,25,25) ppb
T = 295 oK, P = 1 atm.
RH = 95 %

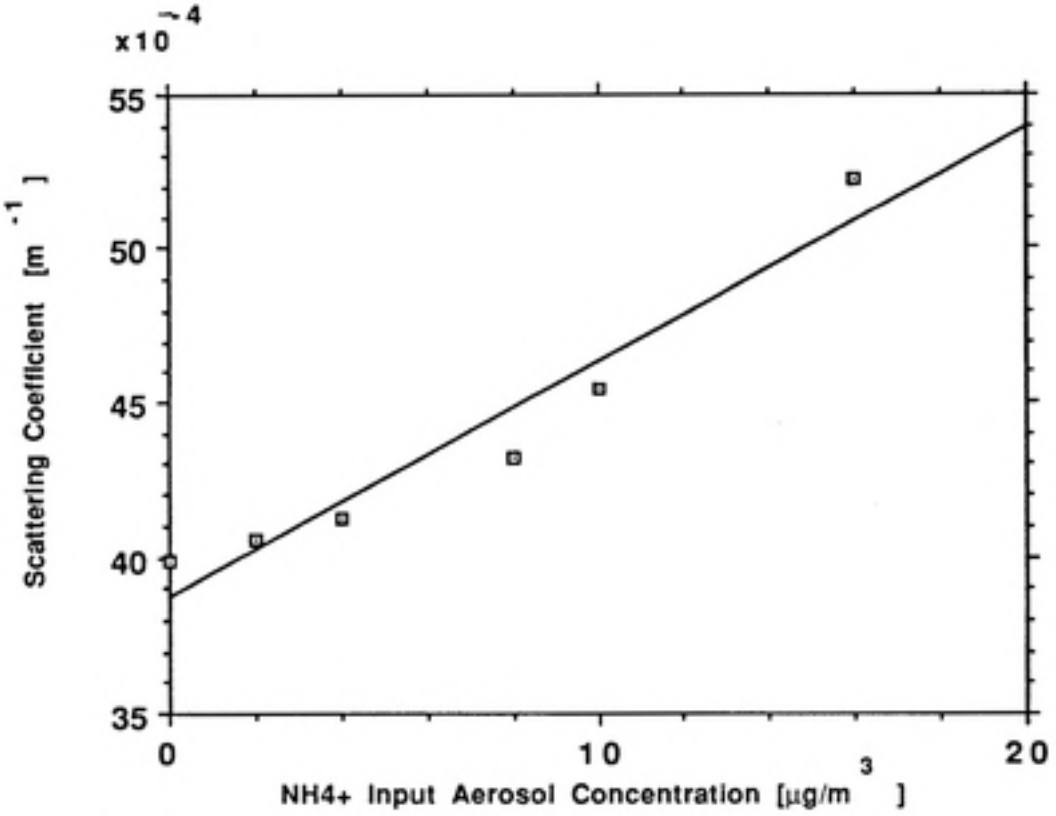
Fig. 12 Scattering coefficient as function of NH4+ aerosol concentration for an ammonia rich environment.



Input Conditions on RWM Simulator to obtain Fig.13:

Index of refraction, m': 1.5
Mean particle diameter (by count)=0.4 µm
Geometric Stand. Dev.= 1.2
Wavelength of light: 0.55 µm
Size Distribution: Log-normal
a = (NH4+,10.7,13.5) µg/m3
B = (10,25,25) ppb
T = 295 oK, P = 1 atm., RH = 95%

Fig. 13 Scattering Coefficient as function of NH4+ aerosol concentration present in the model.



Input Conditions on RWM Simulator to obtain Fig.14:

Index of refraction, m': 1.5
Mean particle diameter (by count)=0.4 µm
Geometric Stand. Dev.= 1.2
Wavelength of light: 0.55 µm
Size Distribution: Log-normal
α = (NH4+,10.7,13.5) µg/m3
B = (50,25,25) ppb
T = 295 oK, P = 1 atm., RH = 95%

Fig. 14 Scattering Coefficient as function of NH4+ aerosol concentration in the model. Ammonia rich environment.

5.3 NEW RESULTS: CRUCIAL TEST

To do a crucial test the RWM program was used to simulate situations in which the aerosol cloud is made up only of one type of chemical or a reduced number of chemicals, all other chemicals being absent. In the process of trying to isolate the effects due to specific chemicals it was found that the RWM program tells us that light scattering behaves surprisingly different when the light beam passes through an ammonia deficient atmoshphere as compared to an ammonia rich atmosphere. By increasing the amount of ammonia ion NH4+ in the atmosphere in an ammonia [NH3] deficient atmosphere, the light scattering coefficient is decreased (Fig.11); on the contrary, if the same simulation is done in an ammonia rich atmosphere, the light scattering coefficient increases (Fig.12). What these simulations tell us is that we have to be very careful when trying to follow up the legislative rules to clean the atmosphere. According to the result of this simulation if, in an ammonia deficient atmosphere, we try to improve the visibility by reducing the amount of NH4+ produced in the atmosphere, the opposite effect can be reached. Fig. 13 shows clearly the

threshold value when in an NH3 deficient atmosphere NH4+ ion is increased. As the NH4+ ion is increased in the model, the scattering coefficient decreases. When NH4+ is increased beyond the calculated value of 12-13 µg/m3, the scattering coefficient starts increasing. Fig. 14 shows the same graph for an NH3 rich atmosphere. Notice that in this case, the scattering coefficient always increases when NH4+ ion is added to the model. In this way, the RWM program provides a new result to be tested by experimental work. If experimental measurements confirm this result, the RWM program would prove to be a useful and resourceful tool for the advancement of science in the area of light scattering. If, on the other hand, the experimental measurements do not confirm the result arrived at by our simulation it would mean that the RWM program has failed to pass the crucial test and the program itself will have to be abandoned or its source code modified to bring it in accordance with the real experimental and theoretical results.

5.4 Relative Visual Index.

According to Koschmieder's theory related to visual range: "There is a relationship between the extinction coefficient (be) and the maximum distance at which an average individual could distinguish an ideal black object silhouetted against the horizon sky"[2] Using this procedure Koschmieder found a relationship that has been

widely used as an indicator of Visual Air Quality, the visual range is given by:

(5) $V = 3.91/be$

There are two basic drawbacks with this definition. First, from the quoted text, the underlined words are subjective. The value of 3.91 is obtained by assuming a value of 0.02 in the relationship $C/Co = \exp(-bex)$, and letting $x=V$ whenever $C/Co=0.02$. The second drawback is that the Visual range for a pristine atmosphere obtained by different investigators differs with each investigator. Seinfeld [31] gives a value of 296 km, Waggoner [39] gives a value of 256 km, Meszaros [4] obtains a value of 335 km, Charlson [3] gives a value of 140 km, Stevens et al. [34] give a value of 190±90_km. To avoid these drawbacks, a new term is defined, the relative visual index defined as follows:

(6) $\eta_V = [b_R(\text{clean air})/b_e(\text{atmosphere})]*100$

Where b_R(clean air) is the Rayleigh scattering.

With this definition, no subjective element is introduced, and the relative visual index for a pristine atmosphere is always 100 %. The relative visual index thus defined is an indication of how clear an object is seen in a polluted environment versus the visual range which gives an indication of how far an object is seen in a polluted

environment. An additional benefit of this definition is that the instrumental errors are minimized. Using Seinfeld's value [31] of $0.132*10^{-4}$ m^{-1} , and Waggoner'value [39] of $0.10*10^{-4}$ m^{-1} for a pristine atmosphere and Charlson et al. data [4], the values for the relative visual index are found (TABLE II). The scattering coefficients (column 1) are the digitize values from Kalkalpen, Austria (values 1 through 13) and from Seattle, Washington (values 13-23) obtained from Fig.4 Ref.[4] (See inset 3). The values in the second column are from the same reference. The values in the third and fifth columns were obtained using relationship (6). Column 4th and 6th were obtained using relationship (7 & 8). Using the experimental relationship given by Charlson et al.[4], be =3.22*Mf with the following units (be[$10^{-4}m^{-1}$],Mf[$\mu g/m^3$] it is obtained 3.22 [m^2/g]}, and the values of bR as given by Seinfeld [29] and Waggoner [37], It is found that:

$$(7)\quad \eta_{v(S)[\%]} = 409/Mf[\mu g/m^3]$$

$$(8)\quad \eta_{v(W)[\%]} = 310/Mf[\mu g/m^3].$$

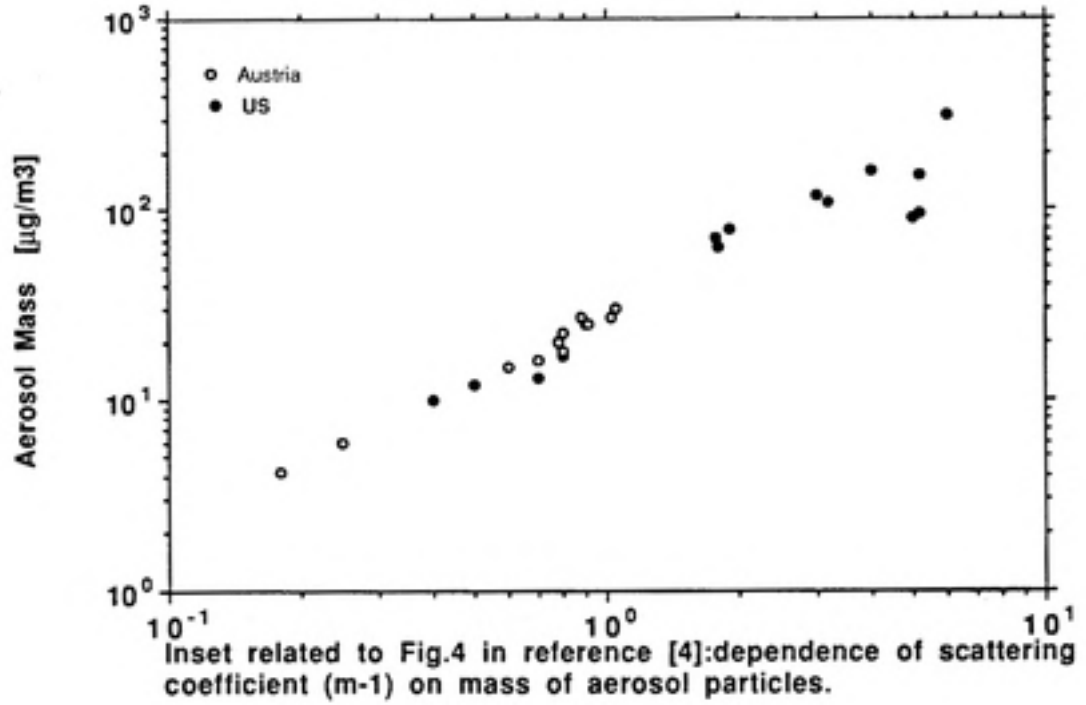
TABLE II. Relative Visual Index obtained using equations (6),(7) and (8).

Value#	be(atmosphere) $(10^{-4}m^{-1})$ (bR)	Mf (µg/m3)	$\eta_{V(S)}$ Eq.(6)&(7) (%)	$\eta_{V(S)}$ Eq.(6)&(7) (%)	$\eta_{V(W)}$ Eq.(6)&(8) (%)	$\eta_{V(W)}$ Eq.(6)&(8) (%)
1	0.18	4.2	73	97	56	74
2	0.25	6	53	68	40	52
3	0.6	15	22	27	17	21
4	0.7	16	19	25	14	19
5	0.8	17	17	24	13	18
6	0.8	18	17	23	13	17
7	0.78	20	17	20	13	15
8	0.8	22	17	19	13	14
9	0.9	25	15	16	11	12
10	0.91	25	14	16	11	12
11	0.88	27	15	15	11	12
12	1.02	27	13	15	10	12
13	1.05	30	13	14	10	10
14	0.4	10	33	41	25	31
15	0.5	12	26	34	20	26
16	0.7	13	19	31	14	24
17	1.8	63	7	7	6	5
18	1.78	71	7	6	6	4
19	1.9	79	7	5	5	4
20	3.2	110	4	4	3	3
21	3.0	120	4	3	3	3
22	5.0	90	3	4	2	3

Sensitivity studies related to η_v

Fig 15a shows the Relative Index of Visibility as calculated using equations (6) and (7). Fig 15b shows the Relative Index of Visibility as calculated using equations (6) and (8). There is no significant difference between the values as calculated using equation (6) and (7), and those using equations (6) and (8). Fig 15a. was obtained using Waggoner's value for Rayleigh scattering. Fig 15b. was obtained using Seinfeld's value for Rayleigh scattering. This tell us that the reference value used for the Rayleigh scattering has as its only effect to shift in a constant amount the calculated values for the relative visual index.

Fig.16 shows the relative visual index as a function of the scattering coefficient (equation 6) for both the Rayleigh scattering as given by Seinfeld and as given by Waggoner. Notice the upward shift in the graph as the Rayleigh scattering is increased from 0.1 (Waggoner's) to 0.132 (Seinfeld's). However, this upward shift may be negligible since it is expected that the same instrument and experimental technique are to be used for the measurement of the Rayleigh scattering and the scattering due to a polluted atmosphere. It can be seen that as the scattering coefficient increases, the relative visual index decreases. Values of the relative visual index of 4% correspond to an aerosol cloud responsible for an scattering coefficient of around 2-3 in units of $[10^{-4}m^{-1}]$.



Inset related to Fig.4 in reference [4]:dependence of scattering coefficient (m-1) on mass of aerosol particles.

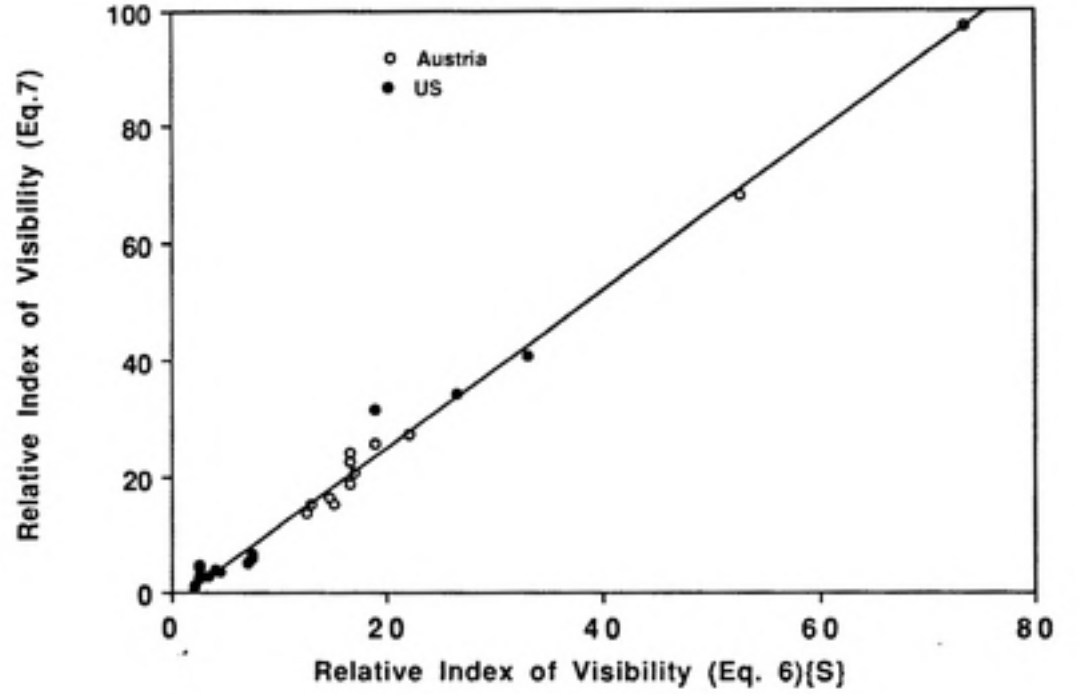
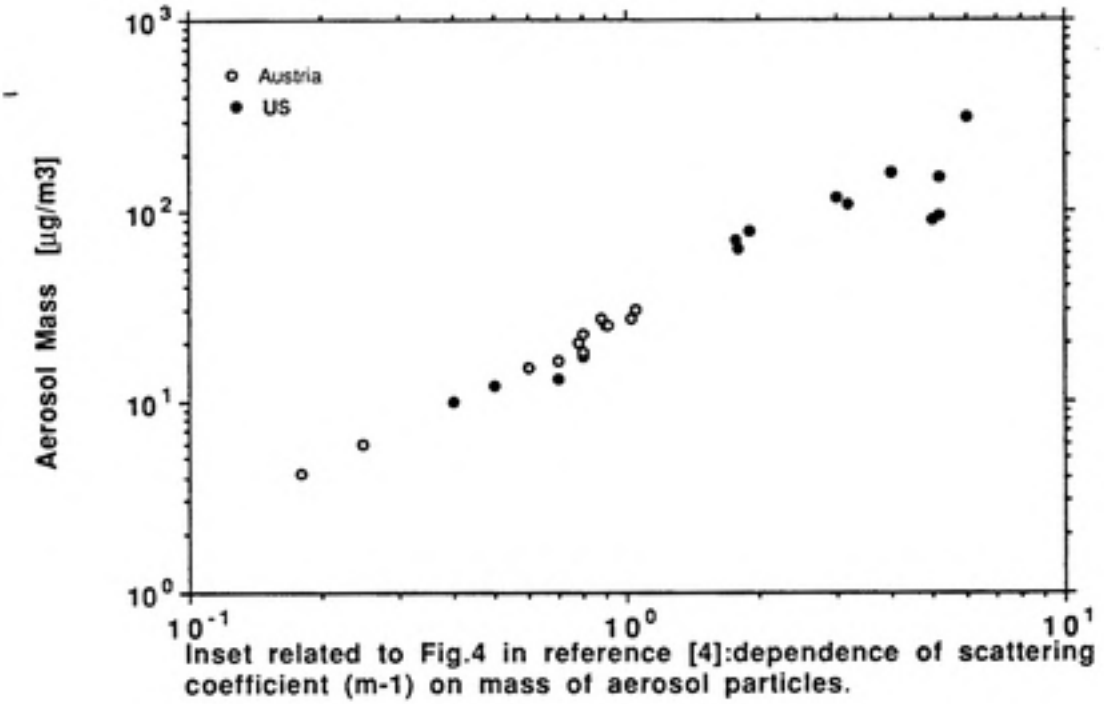


Fig 15a. Comparison of Relative Index of Visibilities using equations (6) and (7) in text.



Inset related to Fig.4 in reference [4]:dependence of scattering coefficient (m-1) on mass of aerosol particles.

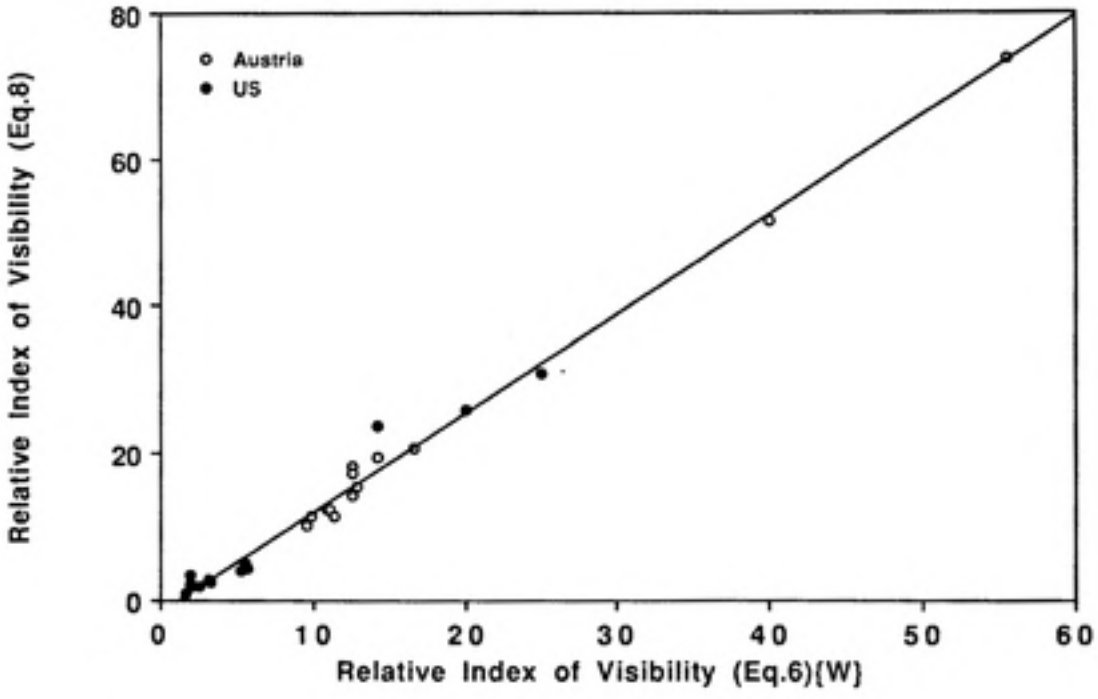
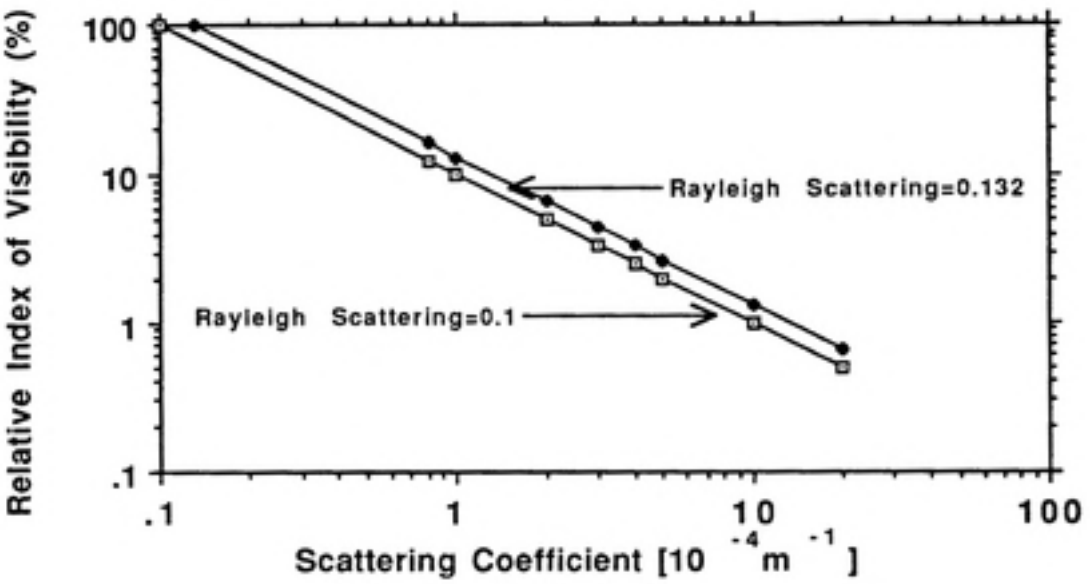


Fig 15b. Comparison of Relative Index of Visibilities using equations (6) and (8) in text.



Relative visual Index [%] η v = [bR/be]x100

Fig. 16 Relative Index of Visibility in % versus extinction coefficient in units of

$[10^{-4}\ m^{-1}]$,

using both values for bR: Seinfeld's and Waggoner's

The lowest value of the relative visual index in a graph of relative visual index as a function of particle diameter occurs in the size range from 0.1 to 1 μm as seen in Fig. 17.

Figures.17-23 is the analysis related to the relative visual index (η_V):

Fig 17.η_V -vs- $\pi dg/\lambda$ corresponding to Fig 1 bms -vs- $\pi dg/\lambda$

Fig 18 η_V -vs-RH corresponding to Fig 3 be -vs- RH .

Fig 19 $\eta_{vs}, \eta_{ve}, \eta_{va}$ -vs-dg.corresponding to Fig 5 bme,bms,bma -vs- dg

Fig 20. η_V -vs-σg corresponding to Fig 5 bms -vs- σg

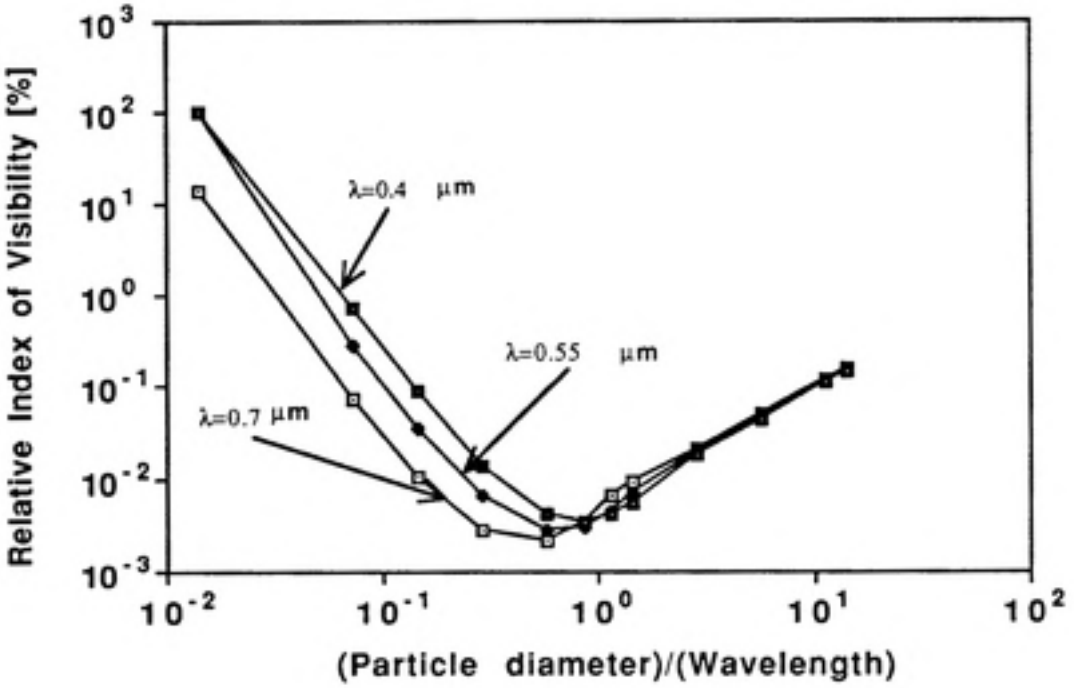
Fig 21.η_V -vs-m'.corresponding to Fig 6 be -vs- m'

Fig 22.η_V -vs-NH_4+ corresponding to Fig 12 bs -vs- NH_4+.

Fig 23.η_V -vs-NH_4+ corresponding to Fig 9.bs -vs-NH_4+

The relative index of visibility reaches a minimum at a value of $\pi d_g/\lambda \approx 1$, as seen in Fig.17. This results correlates well with the result obtained in Fig.1 where the mass scattering coefficient reached a peak at a value of $\pi d_g/\lambda = 1$. That is to say visibility effects are most pronounced for values of particle diameters of the same order of magnitude as the wavelength of the light used for scattering

A very good fit was found between the results as obtained fromt the RWM program for the relative index of visibility versus relative humidity, and the slightly modified theoretical equation as given by Zhang X.Q. as



Relative visual Index [%] η_v = [bR/bs]x100 as a function of the ratio of particle diameter to wavelength of light.

Fig. 17 Relative Index of Visibility in % as a function of the ratio of particle diameter to wavelength of light. The data used for this graph is the same data used for Fig.1.

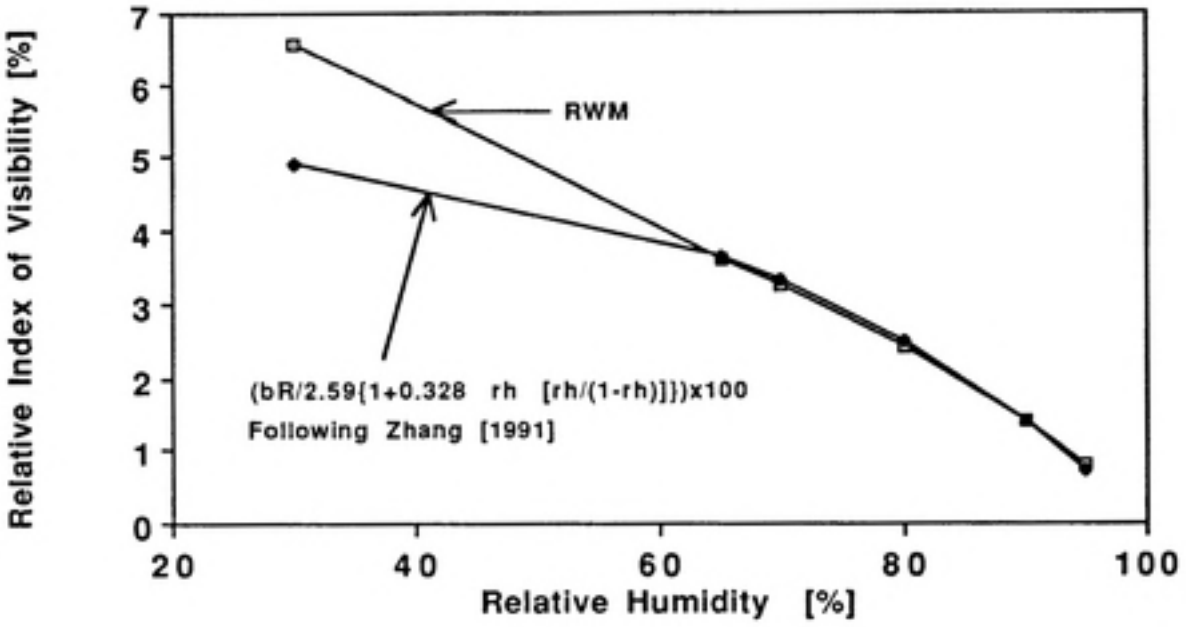
reported in ref [11]. Notice that the fit in both cases Fig.3 and Fig.18 is much better for relative humidities greater than 60 %.

Fig.19 confirms the results obtained in Fig.4. The optically active region is again confirmed to be in the accumulation mode particle range 0.1 to 1.0 μm. The relative index of visibility due to scattering is much less than the relative index of visibility due to absorption, and finally in the nuclei mode particle size range absorption dominates the visibility.

The minimum value of the relative index of visibility occurs for values of the geometric standard deviation between 1.2 to 1.4. As seen in Fig.20. for a dry atmosphere (relative humidity equal to 30 %), the visibility increases considerably, and as the relative humidity increases the visibility deteriorates in agreement with previous results in this technical report (Fig.5)

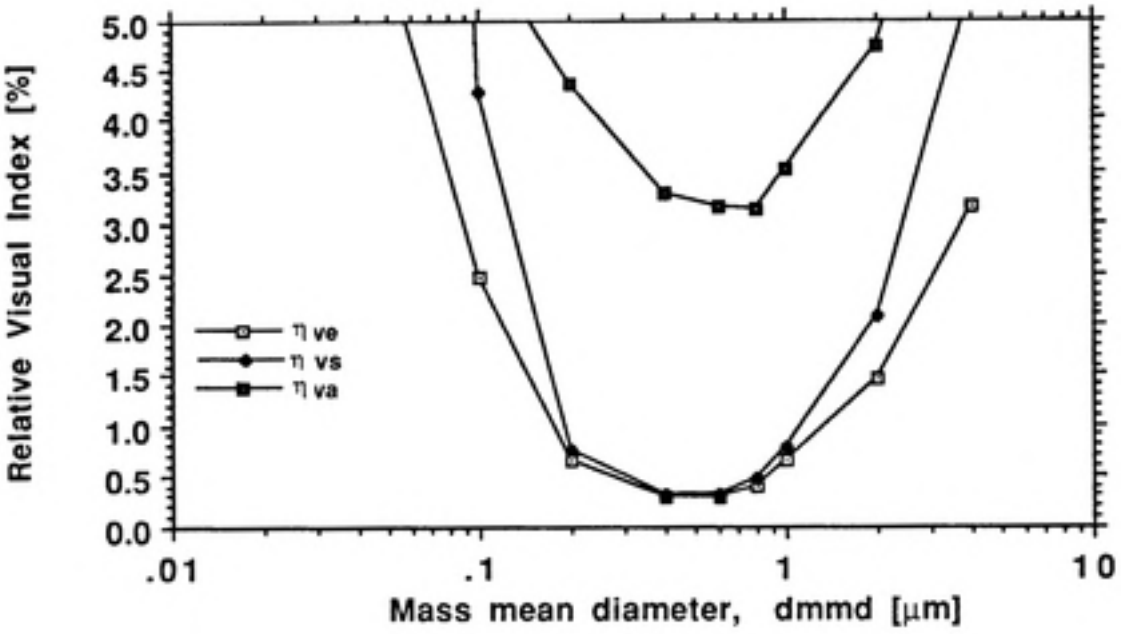
As seen in Fig.21, the relative index of visibility reaches a minimum for values of the index of refraction,m', close to 1.5. This result can be seen more clearly in this figure than in the corresponding equivalent result on Fig.6.

Fig 22 and Fig.23 also confirms results obtained in Fig.11 and Fig.12. In these figures (22 and 23) the relationship between visibility and the increase of NH4+ ion concentration is more clearly seen. As seen in Fig.22, as NH4+ ion concentration increases, the visibility



Relative visual Index [%] η_v = [bR/bs]x100 as a function of relative humidity .

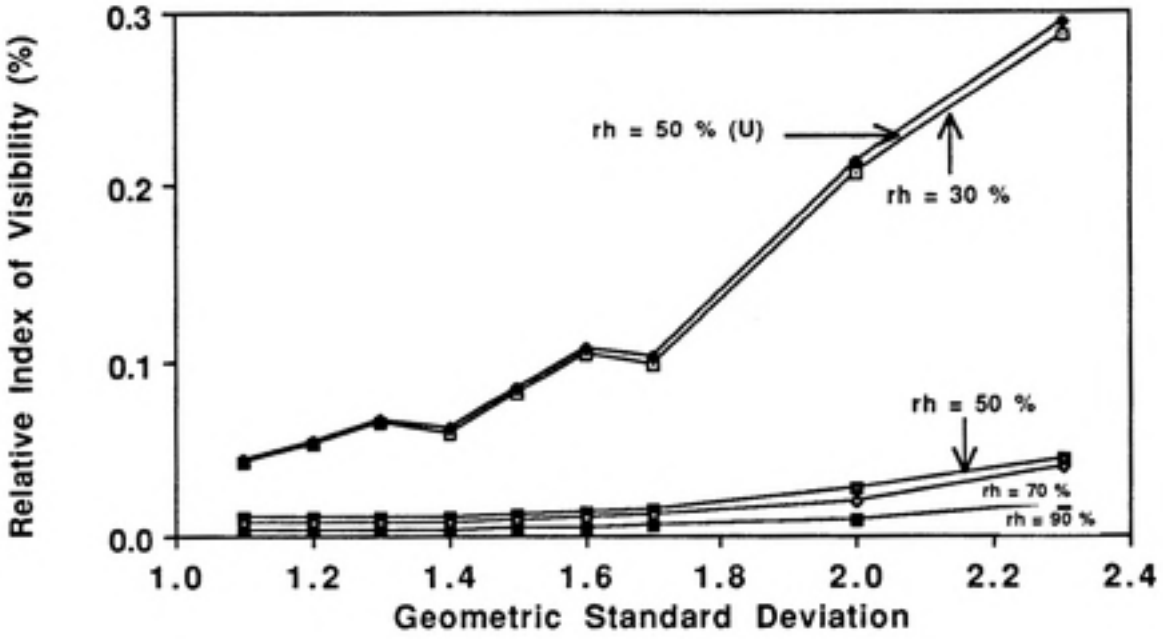
Fig. 18 Relative Index of Visibility in % versus relative humidity in %. The data used for this graph is the same data used for fig. 3.



Relative visual Index [%] η_{vx} = [bR/bx]x100 as a function of mass mean diameter.

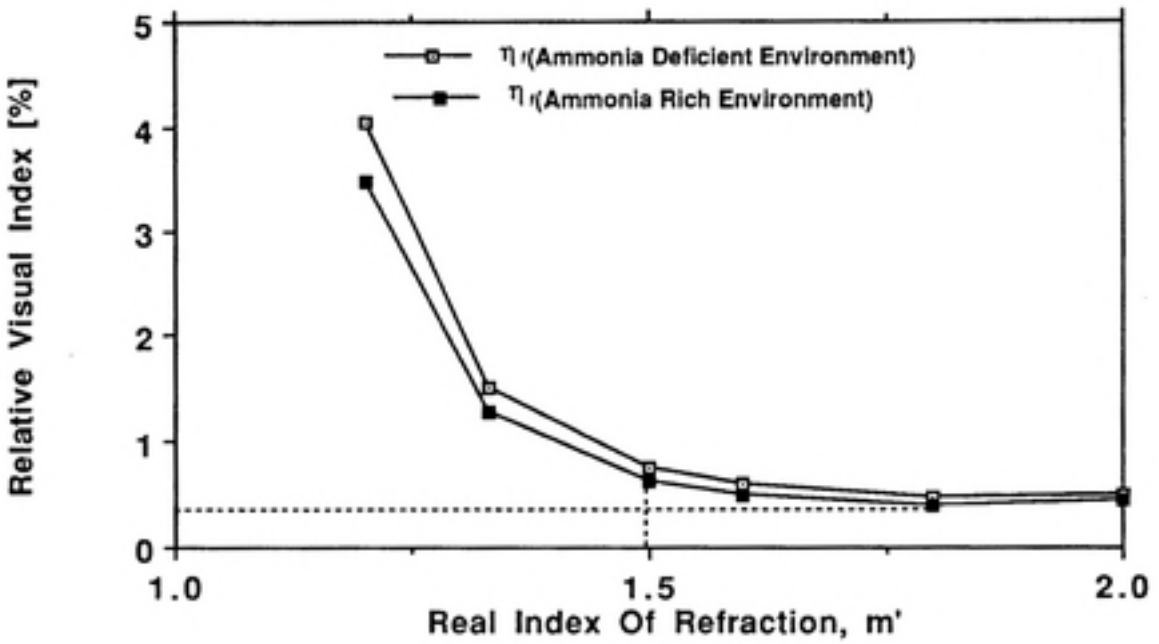
Where x stands for e,s,a

Fig. 19 Relative Index of Visibility in % versus mass mean diameter in μm. The data used for this graph is the same data used for fig. 4.



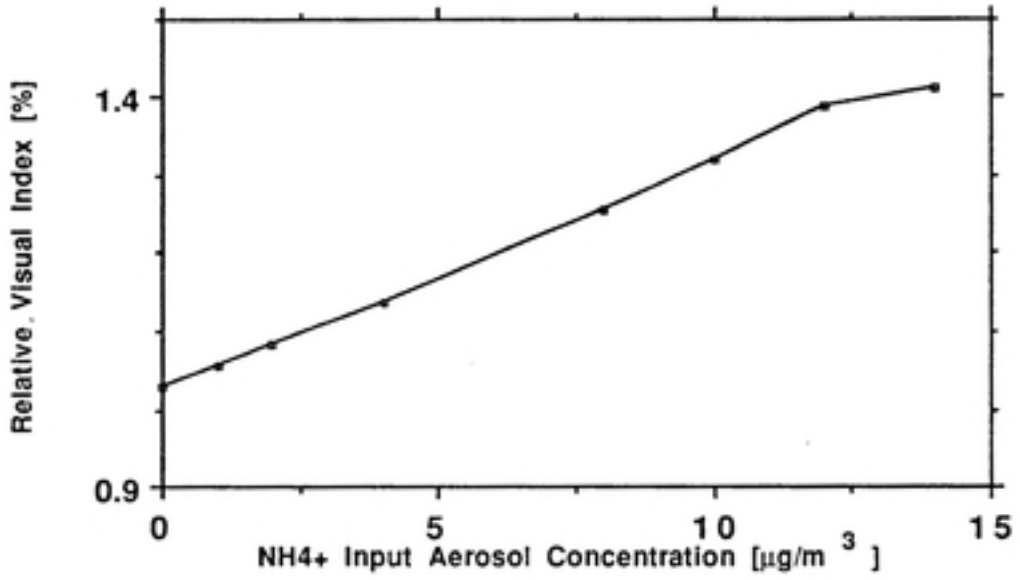
Relative visual Index [%] η_v = [bR/bs]x100 as a function of the geometric standard deviation.

Fig. 20 Relative Index of Visibility in % as a function of the geometric standard deviation. The data used for this graph is the same data used for Fig.5.



Relative visual Index [%] ηv = [bR/be]x100
as a function of m'.

Fig. 21 Relative Index of Visibility in % versus real index of refraction {m'}. The data used for this graph is the same data used for fig. 6.



Relative visual Index [%] η v = [bR/bs]x100 as a function of NH4+ concentration present in the model.

Fig. 22 Relative Index of Visibility in % versus NH4+ aerosol concentration, for an ammonia deficient environment. The data used for this graph is the same data used for fig. 11.

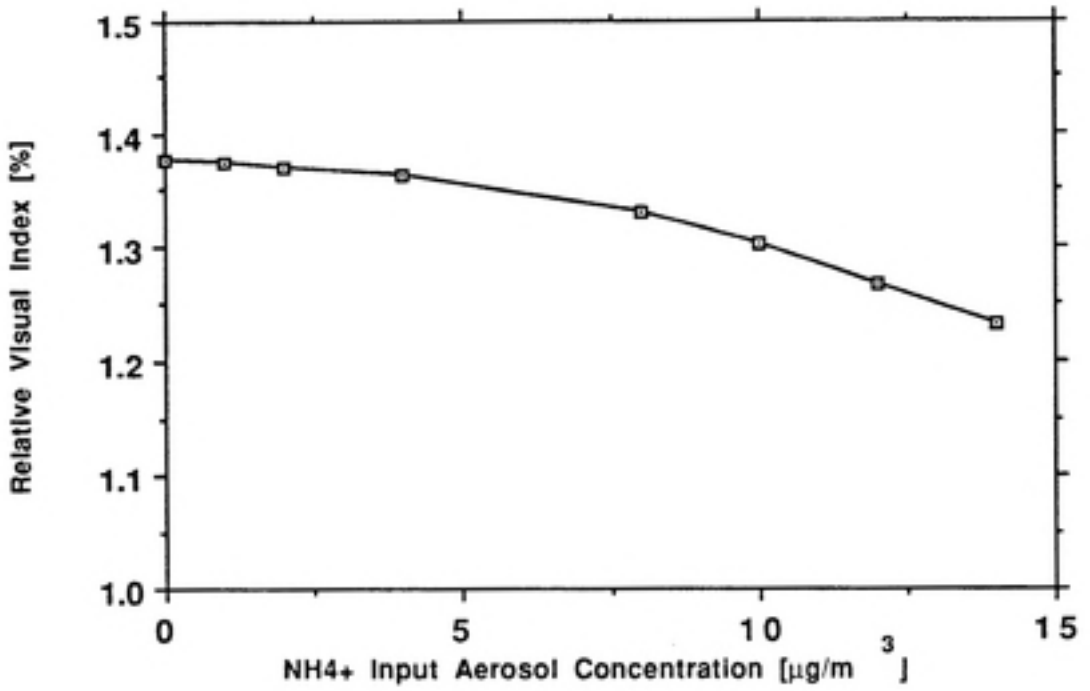
increases. On the other hand, as seen on Fig.23, as the NH4+ ion mass concentration increases, the visibility decreases.

6. CONCLUSIONS

1. The RWM program used to obtain all of our results has proved to be very inexpensive, accesible to most researchers in the field and the output has a high degree of reliability. The RWM program was run in a Zenith Data System 88286/25 Mhz, IBM clone, without the math coprocessor. The printer used was a dot matrix Epson LQ-800. Selective output from the equilibrium results were obtained in hardcopy using the print-screen capabilities.

2. It has been confirmed that the light extinction coefficient is strongly dependent on the relative humidity and on the sulfate mass concentration. As seen on Fig 3 and Fig.6, respectively.

3. It has also been shown that the relationship between visual range (V) and the Total Suspended Particle (TSP) has been modelled into the RWM program. The following relationship has been obtained:



Relative visual Index [%] η_v = [bR/bs]x100 as a function of relative humidity .

Fig. 23 Relative Index of Visibility in % versus NH4+ input aerosol concentration, for an ammonia rich environment. The data used for this graph is the same data used for fig. 12.

V[m] *TSP[μg/m3] = 1.2 g/m2 , r.h.=53%

In good agreement with the empirical relationship found by Charlson [4]. It is suggested on theoretical and experimental grounds that TSP be replaced by the fine mass, Mf. The previous relationship now reads:

V[m]*Mf[μg/m3] = 1.2 g/m2.

4. A crucial test that should be experimentally investigated is how the amount of ammonia ion in the atmosphere relates to the light extinction coefficient. It was found that by increasing the mass concentration of NH4+ component in the RWM model, the model computes a *decrease* in the light extinction coefficient, and therefore an *increase* in the relative index of visibility. If this result is valid, and could be confirmed experimentally, it will be useful in air pollution legislation.

5. It was found that the Relative index of visibility, as an alternative to the Koschmieder relationship can be very effective. A further motivation to look for an alternative relationship to Koschmieder's was the single scattering assumption. If the optical depth is greater than 1, and in particular for an optical depth of 3.91, a value

associated with the Koschmieder relationship, and corresponding to I/Io=0.02, there is the need to make corrections for multiple scattering. In most cases Mie theory is not valid, unless multiple scattering effects happen to be very small and experimentally undetectable. Regardless of the previous comments Mie theory is commonly used for two main reasons: First, during the last fifty years or so, the Mie theory has provided good correlation between theory and experiment. Second, no other theory is available today that gives such good correlation between theoretical and experimental results.

The following TABLE III gives a better comparison between the two alternative ways of describing visibility reduction:

TABLE III. Comparison between the Relative Index of Visibility and the Visual Range.

name:	Visual Range	Relative Index of Visibility
Symbol:	V	η_v
Formula:	V = 3.91/be	η_v = (bR/be)*100%
Units:	[km]	[%]
Conceptual Terms :	How Far	How clear
Values:	In both cases the smaller the values the greater the pollution	

5. It was found that the RWM program is very efficient at being able to reproduce well known experimental and theoretical results in the field of scattering by small particles. This result in itself is found remarkable in view of the fact that the RWM program code is based on the Mie scattering theory, and the Mie theory deals with an ideal aerosol.

8. APPENDIX A: Conversion Factors. Units (Using ideal gas law constants)

The µg/m3 to ppb conversion equation is:

(B1) $[Ci]ppb = 0.041*Mi*[Ci]\ \mu g/m3$

While the ppb to µg/m3 conversion can be done with equation:

(B2) $[Ci]\mu g/m3 = (24.45/Mi)*[Ci]ppb$

Relationships (B1) and (B2) were obtained at a $T=298^{o}K$ and P = 1,013 mb.
Where Mi is the molecular concentration of the given compound.

12. APPENDIX B: Acute Effects.

Unluckily for life on earth visibility reduction is not only a question of aesthetics, though it can be argued that lack of aesthetics will render life on this planet useless. Visibility reduction has produced in the past and might produce in the future some rather nasty and acute effects. During the 1980's the nuclear winter theory was proposed by several scientists [18,21] as a means of bringing some measure of sanity and hopefully control, on the nuclear proliferation program of the US and the USSR. During the same period other scientists (See for example Alvarez and Asaro, Scientific American, October 1990, pp78-95) explained the disappearance of the dinosaurs some 60 million years ago by mean of two opposing theories: the meteorite shower theory and the volcanic eruption hypothesis. Whatever the final outcome on the validity of these two theories, both theories relied on the onset of an ice age on the planet due to visibility degradation. More mundane effects but just as acute are being reported on a yearly basis as is evident from newspaper accounts during the last few years.

In the mean time the fact that visibility degradation is thought mostly as a "nuisance" effect [40], i.e., as a by product of aerosol pollution and not as a real threat to the well being of life on earth, is the main reason behind its classification as a secondary ambient air quality standard. However what today is classified as a secondary pollutant, might be classified tomorrow as a primary pollutant. Several of the most vivid and dramatic cases in which this legislation has been put to the test follows: Indiana "Heavy fog forced the closure of an eastbound section of I-74 in Indiana after 30 cars pile up in January 28, 1991. "[14] California: "A sudden, blinding dust storm trapped hundredths of holiday motorists on Interstate 5 in the San Joaquin Valley on November 29, 1991, leaving at least 19 people dead and 114 injured in a series of chain reaction accidents, the California highway patrol said."[15]. Tennessee: Heavy fog causes multiple crash on highway I-75 between Knoxville and Tuscaloosa. Again California: "A California highway patrol cruiser, stopped in traffic lanes as an officer place flares at a suspected drunk driving accident was rear-ended by another car, setting off a chain reaction pile up under a blanket of fog on Interstate 15 near Rancho Cugamunga, California on October 18,1992, authorities said."[16] , and "Big-rig trucks, cars and a school bus piled into each other in a 94 vehicle wreck on a fog bound mountain in California

interstate on March 20, 1990 killing one person and injuring 46." [17] To all these accidents and several others, some authorities are **blaming the drivers** as seen in the following announcement "The National Transportation Safety Board found on September 28, 1992 that a phenomenon it calls **non-uniform driver response** was to blame for six multi-vehicle highway pile ups in fogs and dust in 1991."[35] However, part of the scientific answer for these accidents was given by a reporter to the New York Times writing about the Mexican air pollution occurrence of 1992: "Mexico city is blanketed by growing brown smog even more dangerous than usual, forcing government to close down schools, curb factory output and ban almost all cars from streets, ...vast city full of cars burning leaded gasoline is, even more than Los Angeles, ringed by mountains that trap smog during **regular thermal inversions**, when there is almost no wind."[35] Thermal inversion takes place through cooling from below or heating from above. All the previously quoted accidents - except the one in California due to the "blinding dust storm" took place due to ground based inversions. In these cases, the temperature increases with height, the troposphere is very stable and all vertical motions are suppressed. The New York Times reporter was right: during an Inversion there is almost no wind to help disperse the fog. Ironically, the other case mentioned above and not explained by thermal

inversion, took place due to a high wind that was responsible for bringing aerosol dust from a desert region and blanketed interstate 5 in the San Joaquin Valley. A secondary ambient air quality standard was responsible for effects of a primary ambient air quality standard.

15. REFERENCES

[1] Bergstrom, R.W.,Babson B.L., and Ackerman T.P., "Calculation of multiply-scattered radiation in clean atmospheres," Atmospheric Environment, 15 :1821-1826, (1981).

[2] Private Communication.

[3] Cass G.R., "On the relationship between sulfate air quality and visibility with examples in Los Angeles," Atmospheric Environment 13:1069-1084,(1979).

[4] Charlson R.J., Horvath H., and Pueschel R.F., "The direct measurement of atmospheric light scattering coefficient for studies of visibility and pollution," Atmospheric Environment 1:469-478,(1967).

[5] Crump, G.J.,and Seinfeld J.H., "A New Algorithm for Inversion of Aerosol Size Distribution Data," Aerosol Science and Technology, 15-34 (1982).

[6] Fox D.G., Rosenthal D., "On the use of decision Analysis in determining significant visibility impairment," Atmospheric Environment,15:2503-2510,(1981).

[7] Groblicki P.J., Wolff G.T. , and Countess R.J., "Visibility Reducing Species in the Denver Brown Cloud_ I. Relationships Between Extinction and Chemical Composition," AtmosphericEnvironment15:2473-2484,(1981).

[8] Horvath H., "Atmospheric Light Absorption.- A Review,"Atmospheric Environment, 27A:293-317,(1992).

[9] Horvath H., "Atmospheric Visibility," Atmospheric Environment,15:1785-1796,(1981).

[10] Jaggard D.L., Hill C., Shorthill R.W., Stuart D.,Glanz M., Rosswog F.,Taggart B., and Hammond S., "Light Scattering from Particles of Regular and Irregular Shape," Atmospheric Environment, 15: 2511-2519,(1981).

[11] Laulainen, N.S.,"Summary of Conclusions and Recommendations from a Visibility Science Workshop", April 1993. Pacific Northwest Laboratory. Richland, Washington 99352.

[12] Lewis,C.W.,"On The Proportionality of Fine Mass Concentration and Extinction Coefficient for Bimodal Size Distributions", Atmospheric Environment, 15:2639-2646,(1981).

[13] Lewis,C.W.,and Dzubay T.G., "Measurement of Light Absorption Extinction in Denver," Aerosol Science and Technology, 5:325-336,(1986).

[14] Los Angeles Times Index, (1992) pp 1805

[15] Los Angeles Times Index, (1992) pp 1805

[16] Los Angeles Times Index, (1992) pp 1606

[17] Los Angeles Times Index, (1992) pp 1606

[18] MacAdam, D.L., "Perceptual Significance of Colorimetric Data for Colors of Plumes and Haze," Atmospheric Environment, 15:1797-1803,(1981).

[19] Middleton, P., and Kiang, C.S., "A Kinetic Aerosol Model For The Formation And Growth Of Secondary Sulfuric Acid Particles," J. Aerosol Science 9:359-385,(1978).

[20] Nair P.V.N., "Growth of Particles of Mixed Composition in the Atmosphere as a Function of the Relative Humidity," J. Aerosol Science 19:849-852,(1988).

[21] Nelson, J., "Fractality of Sooty Smoke: Implications for the Severity of Nuclear Winter," Nature, 339:611-613,(1989).

[22] New York Times Index, (1992) pp 28

[23] Ortiz J.L., Apablaza N., Campos C., Zolezzi S., and Prendez M., "Tropospheric Aerosols Above the Thermal Inversion Layer of Santiago, Chile:Size Distribution of Elemental Concentrations," Atmospheric Environment, 27A:397-399,(1993).

[24] Ouimette J.R., and Flagan R.C., "The Extinction Coefficient of Multi Component Aerosols.," Atmospheric Environment 16:2415-2419,(1982).

[25] Pilinis C., Seinfeld J.H., and Seigneur C., "Mathematical Modeling of the Dynamics of Multicomponent Atmospheric Aerosols," Atmospheric Environment, 21:943-955,(1987).

[26] Pilinis C., and Seinfeld J.H., "Continued Development of a General Equilibrium Model for Inorganic Multicomponent Atmospheric Aerosols," Atmospheric Environment, 21:2453-2466,(1987).

[27]Raabe, G. O., "Particle Size Analysis utilizing group data and the Log-Normal Distribution," Aerosol Science 289-303 (1971)

[28] Reist P.C., "Users Manual. General Notes and documentation. Program for studying the influence of particle composition and light scattering as a function of relative humidity," (1993).

[29] Reist P.C., Physics of Aerosol Science

[30] Saxena P., Hudischewskyj A.B., and Seigneur C., "A Comparative Study of Equilibrium Approaches to the Chemical Characterization of Secondary Aerosols," Atmospheric Environment, 20:1471-1483, (1986).

[31] Seinfeld, J.H. , Atmospheric Chemistry and Physics of Air Pollution, chapter 7, John Wiley & Sons, New York (1986).

[32] Sloane C.S. (1988). Contribution of NO2 and Soot to the discoloration of urban skies. Atmospheirc Environment 22, 2021-2031.

[33] Stelson A.W., and Seinfeld J.H., "Thermodynamic Predictions of the Water Activity, NH_4NO_3 Dissociation Constant, Density and Refractive Index for the NH_4NO_3-$(NH_4)_2SO_4$-H_2O System at 25oC," Atmospheric Environment, 16:2507- 2514,(1982).

[34] Stevens R. K., Dzubay T. G.,Russwurm G., and Rickel D. "Sampling and Analysis of Atmospheric Sulfates and Related Species" Atmospheric Environment, 12, 55-68 (1978)

[35] The Washington Post Index, (1992) pp 1627

[36] Tsay S, Stephens G.L.,and Greenwald T.J., "An Investigation of Aerosol Microstructure on Visual Air Quality," Atmospheric Environment, 25A:1039-1053, (1991).

[37] Trier A., and Horvath H., "A Study of the Aerosol of Santiago de Chile-II. Mass Extinction Coefficients, Visibilities and Ångstrom Exponents," Atmospheric Environment, 27A:385-395,(1993).

[38] Van de Hulst H.C., Light Scattering by Small Particles, chapter 9 Wiley, New York (1957)

[39] Waggoner A.P., Weiss R.E.,Ahlquist N.C., Covert D.S., Will S., and Charlson R.J., "Optical Characteristics of Atmospheric Aerosols," Atmospheric Environment, 15:1891-1909,(1981).

[40] Wayne R.P. ,Chemistry of Atmospheres, Clarendon Press,(1992).

[41] Went F.W., "Blue Hazes in the Atmosphere," Nature, 4738:641-643,(1960).

[42] White W.H., and Roberts P.T., "On the Nature and Origins of Visibility Reducing Aerosols in the Los Angeles Air Basin," Atmospheric Environment, 11:803-812,(1977).

LIST OF TABLES

Page

TABLE I. Trace Species concentrations in the clean troposphere and polluted urban air.....14

TABLE II. Digitized scattering coefficients and fine mass from reference [4] and computed relative visual indexes using equations (6),(7) & (8).....40

TABLE III. Comparison of Visual Range and Relative Index of Visibility.....56

LIST OF FIGURES

Page

FIGURE A. Block Diagram for the relationship between simulated theoretical and experimental 3

FIGURE 1. Mass Scattering Coefficient as a function of the ratio of particle diameter to wavelength of light.16

FIGURE 2. Mass Extinction Coefficient as a function of the particle diameter for different values of index of refraction 18

FIGURE 3. Scattering Coefficient as a function of the relative humidity.....19

FIGURE 4. Mass Extinction, absorption, and scattering coefficients as a function of particle diameter.....21

FIGURE 5. Mass Scattering Coefficient as a function of the geometric standard deviation.....22

FIGURE 6. Scattering coefficients as function of real index of refraction.....25

FIGURE 7. Extinction coefficients as function of total suspended particles 26

FIGURE 8. Mass Extinction Coefficient as function of sulfate concentration 28

FIGURE 9. Extinction Coefficient as function of nitrate concentration 29

FIGURE 10. Extinction Coefficient as function of carbon concentration 30

FIGURE 11. Scattering coefficient as function of NH_4^+ concentration for an ammonia deficient environment....31

FIGURE 12. Scattering coefficient as function of NH_4^+ concentration for an ammonia rich environment.....33

FIGURE 13. Scattering coefficient as function of NH_4^+ concentration for an ammonia deficient environment....31

FIGURE 14. Scattering Coefficient as a function of the NH_4^+ input concentration to the model 35

FIGURE 15a.Comparison of Relative Index of Visibilities using equations (6) and (7) in text.....42

FIGURE 15b.Comparison of Relative Index of Visibilities using equations (6) and (8) in text.....43

FIGURE 16.Relative Index of Visibility as a function of the extinction coefficient.....44

FIGURE 17. Relative Index of Visibility as a function of the ratio of particle diameter to wavelength of light.....46

FIGURE 18.Relative Index of Visibility as function of relative humidity.....48

FIGURE 19.Relative Index of Visibility as function of mass mean diameter 49

FIGURE 20.Relative Index of Visibility as function of the geometric standard deviation.....50

FIGURE 21. Relative Index of Visibility as function of real index of refraction 51

FIGURE 22.Relative Index of Visibility as function of NH_4^+ concentration for an ammonia deficient environment.....52

FIGURE 23.Relative Index of Visibility as function of NH_4^+ concentration for an ammonia rich environment.....54

SYMBOLS AND ABBREVIATIONS.

bs : scattering coefficient in [$10^{-4}m^{-1}$].

ba : absorption coefficient in [$10^{-4}m^{-1}$].

be : extinction coefficient in [$10^{-4}m^{-1}$].
for a polydisperse system

σep : extinction coefficient for a single particle.

Qe : efficiency factor.

bms : mass scattering coefficient in [m^2/g].

bma : mass absorption coefficient in [m^2/g].

bme : mass extinction coefficient in [m^2/g].

α = Aerosol Phase (NH4+,NO3-,SO4=),in [µg/m3].

β = Gas Phase (NH3,HNO3,H2SO4), in [ppb].

Dg : geometric diameter by count in [µm].

Dmmd: mass mean diameter in [µm].

σ_g : geometric standard deviation.

m' : Index of refraction.

mi : aerosol concentration of compound i [µg/m3]

Mi : Molecular weight of compound i in [g].

V : Visual Range in [m].

η_V: Relative Visual Index in [%].

τ : Optical Depth.

TSP: Total Suspended aerosol Particles concentration in [$\mu g/m^3$].

Mf : Fine or accumulation mass in [$\mu g/m^3$]

ppb: Parts Per billion.

Io: Intensity of incident (incoming) light beam in [watts/m^2]

I : Intensity of outgoing light beam in [watts/m^2].

1. INTRODUCTION

This paper reports on a test of the effectiveness of the Reist Wilson Mars (RWM) program to calculate scattering efficiency values of particulate matter formed from chemical reactions in the atmosphere. The test of the program was done in a two level approach taking into consideration the relationship between simulation, theory, and experimental work as described in the methodology section. The first level was designed as an exhaustive test and only after the program satisfied the requirements of this initial test was the second level attempted which was called a crucial test.

Methodology

To test the program in an exhaustive way, major results and hypotheses related to visibility reduction were searched throughout the literature. Then, simulations were run using the RWM program under conditions similar to the ones found in the literature for the specific findings. Finally,

comparisons were done between the RWM results and the previously published results.

To provide a crucial test of the RWM program, simulations of the RWM program under extreme experimental conditions were designed and run. It was found that the simulation itself was able to suggest insights to the experimentalist. This could be used to assist in the interpretation of new results in the behavior of the light scattering coefficients as it relates to the fractional mass concentration.

Relationship between simulated, theoretical and Experimental work

The relationship between theory, experiment and simulated work is better explained through a block diagram (FIG.A). Since the 1980's when the PC came in full force, scientists have been replacing the proverbial "thought experiment" with "virtual experiments". Today experiments are "performed" and answers are obtained using a computer program. In this way, computer simulation is a test of a theory, and it is hoped that a good simulator can discriminate between a well-founded approach to a problem and merely a speculative suggestion of a less than plausible outcome. In this technical report it was one of our aims to develop a crucial test for the simulation, where crucial was meant to be a new or not yet found result that could give experimentalists and

theorist alike some job to do. The simulator is a bridge between the theory and the experiment, making the theory more accessible to experimentalist and vice versa.

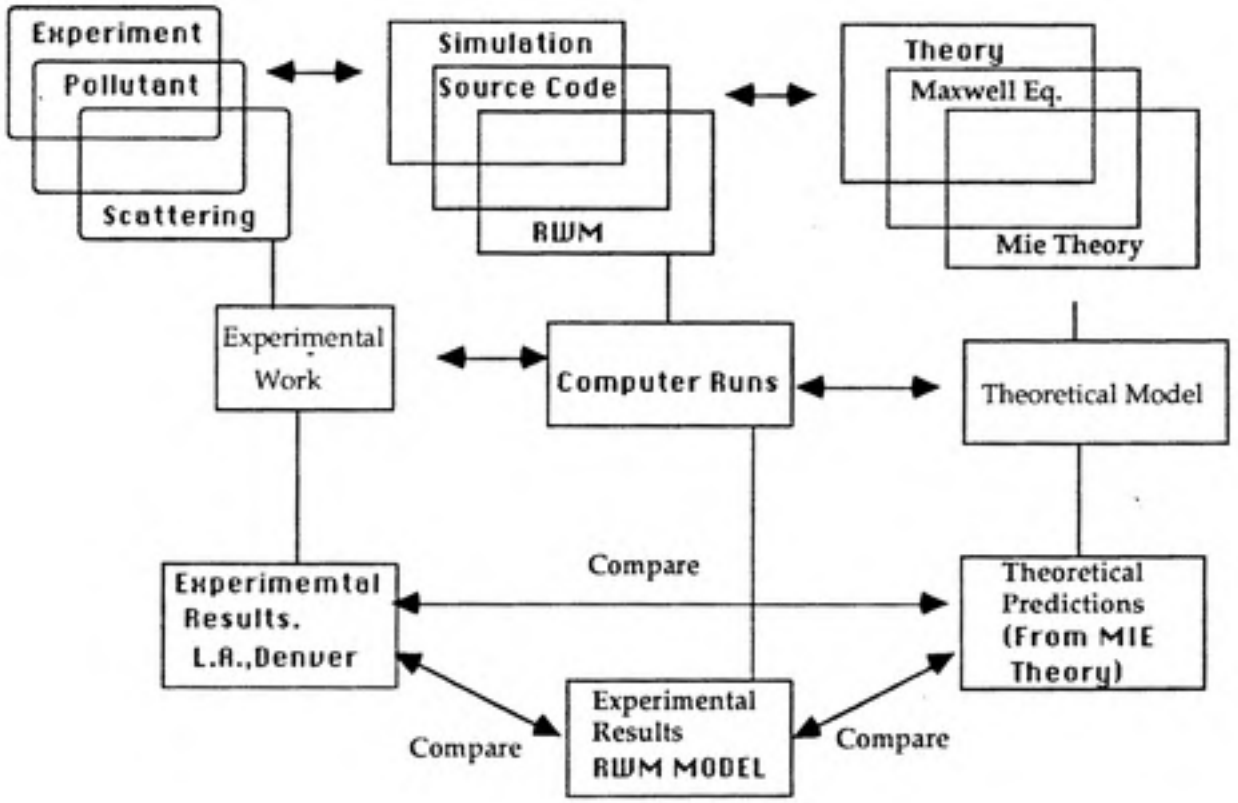


FIG.A. Block diagram showing the relationship among the different elements that are considered in this technical report: The experimental work, the RWM simulator and the MIE scattering theory.

3. THEORETICAL BACKGROUND

Visibility reduction is due to the interaction of light with matter, giving rise to absorption and scattering. The results of this technical report will be based on the framework of the Mie scattering theory, which predicts the interaction of light with small particles.
This report then rests on Mie's theory basic assumptions [38]:

3.1 Basic Assumptions

The basic assumptions associated with MIE theory are as follows:

i) Elastic interaction between light and matter.

ii) Independence of the particles.

iii)Single Scattering.

iv) Sphericity of the particles.

v) The same index of refraction for all the aerosol. These assumptions are discussed in more detail below:

i) All the interaction of light with matter is elastic. The incoming and outgoing photons have the same frequency f'=f. Inelastic scattering takes place when there is some electron transition between energy levels giving rise to Raman scattering and other quantum effects. The spectrum

of the visible radiation that this report deals with does not have enough energy to produce inelastic scattering. Thus, this is a valid assumption for the interaction of visible light with aerosols.

ii) The distance between the particles is greater than 3 times the radius. The radiation of one particle is independent from another one. The phase relation among the different scattering centers is random. This means that there is not a phase or a cooperative effect. A cooperative effect is one that takes place when phase coherence phenomena occurs. This is also a valid assumption.

iii) The effects of multiple scattering will be neglected. This is the most restrictive assumption, since with observed results in the atmosphere there usually is multiple scattering. If the optical depth ($\tau=\sigma_e x$), is less than 0.1($\tau<0.1$) single scattering prevails [38]. This corresponds to cases where the ratio of $I/Io>0.9$. In the expression $\sigma_e x$, σ_e is the cross section extinction coefficient, and x is the optical distance travelled by the light beam. If the optical depth is between 0.1 and 0.3 ($0.1<\tau<0.3$), corresponding to $0.90 > I/Io > 0.74$, it may be necessary to make corrections for double scattering [38].

iv) Extinction coefficients by regularly and irregularly shaped particles have been reported in the Iiterature [10]. The RWM program does not consider these cases. It only takes into consideration spherical particles. For the size of the particles being considered, which are of the same order of magnitude as the visible light, the shape of the particle might not have a very profound effect. Since $x= \pi d/\lambda=1$, the wavelength of the visible light will envelope the entire particle.

v) All aerosol particles have the same index of refraction. This assumption is also a bit restrictive since the different aerosol compounds have indexes of refraction in the range of 1.2 to 1.72.

3.2 Mie Theory. Extinction Coefficient.

The extinction coefficient for a single particle of radius r is given by Van de Hulst [38],pp 127 as:

$$(1) \quad \sigma_{ep} = \pi r^2 Q_e$$

where Q_e is the efficiency factor developed by Mie using electromagnetic theory for the incident wave being scattered by a spherical homogeneous particle. The efficiency factor Q_e depends on the size parameter x